

1970

Large, multilayer, high density, nondestructive readout film memories

Howard Emil Krohn
Iowa State University

Follow this and additional works at: <https://lib.dr.iastate.edu/rtd>

 Part of the [Electrical and Electronics Commons](#)

Recommended Citation

Krohn, Howard Emil, "Large, multilayer, high density, nondestructive readout film memories " (1970). *Retrospective Theses and Dissertations*. 4852.
<https://lib.dr.iastate.edu/rtd/4852>

This Dissertation is brought to you for free and open access by the Iowa State University Capstones, Theses and Dissertations at Iowa State University Digital Repository. It has been accepted for inclusion in Retrospective Theses and Dissertations by an authorized administrator of Iowa State University Digital Repository. For more information, please contact digirep@iastate.edu.

71-14,240

KROHN, Howard Emil, 1939-
LARGE, MULTILAYER, HIGH DENSITY, NONDESTRUCTIVE
READOUT FILM MEMORIES.

Iowa State University, Ph.D., 1970
Engineering, electrical

University Microfilms, A XEROX Company, Ann Arbor, Michigan

LARGE, MULTILAYER, HIGH DENSITY, NONDESTRUCTIVE
READOUT FILM MEMORIES

by

Howard Emil Krohn

A Dissertation Submitted to the
Graduate Faculty in Partial Fulfillment of
The Requirements for the Degree of
DOCTOR OF PHILOSOPHY

Major Subject: Electrical Engineering

Approved:

Signature was redacted for privacy.

In Charge of Major Work

Signature was redacted for privacy.

Head of Major Department

Signature was redacted for privacy.

Dean of Graduate College

Iowa State University
Ames, Iowa

1970

TABLE OF CONTENTS

	Page
INTRODUCTION	1
LITERATURE REVIEW	3
MEMORY STORAGE ELEMENT	4
Operating Principles	4
Fabrication Considerations	7
EXPERIMENTAL EQUIPMENT AND FABRICATION RESULTS	12
NDRO Memory Tester	12
Evaporation Procedure	15
Array Fabrication	17
LARGE MEMORY DESIGN	38
Introduction	38
Memory Array	38
Design Considerations	41
Test System	44
Word Line Selection	46
Digit Drivers and Sense Amplifiers	50
Measurements	55
DISCUSSION AND CONCLUSION	63
ACKNOWLEDGMENTS	64
REFERENCES	65

INTRODUCTION

Magnetic planar thin films have been used in destructive and nondestructive readout memories for a number of years. DRO film memories have found limited application as scratch pad and control memories¹⁻⁴ while NDRO memories have been used in several commercial and aerospace computer applications.⁵⁻¹¹ If film memories are to remain active in computer applications they must not only have good performance characteristics but they must provide lower storage cost. In order to achieve this goal higher bit densities, lower drive currents, economic array fabrication and inexpensive plane wiring must be achieved.

Magnetic memories have dominated scratch pad and control memory applications however batch fabricated semiconductor memories should slowly replace them in the coming years. The ease at which logic designers can implement semiconductor memories and their cost competitiveness should speed this transaction. Magnetic memories will continue to be used in applications requiring nonvolatile storage and in bulk storage applications where they should remain cost competitive.

Aerospace processors and commercial digital equipment have obvious requirements for NDRO electrically alterable memories. Computer installations require mass storage facilities for library routines and data files needing little change. Aerospace processors implement NDRO memories

that are loaded by ground support equipment and then read during flight.

Previously constructed NDRO magnetic film memories have reasonable bit densities but require large drive currents or have low output signals.⁵⁻¹¹ It is the intent of this study to show that high density NDRO memory arrays can easily be fabricated with existing techniques. These arrays will have output signals of 1.0 mV to 1.5 mV, read currents of 70 mA with 30 nsec rise time and write, digit currents of 250 mA and 45 mA respectively. It will also be shown that these memory arrays can be used in bulk memory applications with adequate operating margins.

LITERATURE REVIEW

Numerous investigators have proposed using coupled planar thin films to overcome demagnetizing effects and thus achieve denser magnetic thin film memory arrays. Raffel, Crowther and Chang have investigated the use of closed flux coupled film elements.^{1,12,13} Raffel and Crowther have suggested the use of small, high coercive force film elements.^{11,12} A process for batch fabricating multilayer film arrays was described by Bertelsen.¹⁴ The properties of coupled films have been investigated by several authors.¹⁵⁻¹⁸

In 1959 Oakland and Rossing noted how a high coercivity data film and a low coercivity sensing film can be combined to form a single NDRO storage element.⁶ Control Data Corporation has constructed NDRO film memories using similar coupled films.⁷ Pohm has shown how high and low coercive force coupled films can be used in a $.25 \times 10^6$ NDRO memory to achieve compatibility with integrated circuits.¹⁰

Matched coupled films have been used to produce NDRO memories. Janisch achieved NDRO storage using a drive line and its ground plane image to switch the read film but not the storage film.⁵ Kohn also uses matched coupled films for nondestructive storage.⁹

MEMORY STORAGE ELEMENT

Operating Principles

The memory storage element investigated is essentially an outgrowth of NDRO storage elements discussed in the literature. The storage element, depicted in Figure 1, consists of a sense/digit line positioned between a high coercive force storage film and a low coercive force data film. Easy axis flux closure and mechanically defined film strips allow close sense/digit line spacing.

Reading and writing are accomplished by means of drive fields produced by currents flowing in orthogonal word and digit lines passing over and between coupled films. Digit field is applied parallel to the easy axis and word field is applied perpendicular to the easy axis.

Figure 2 shows the basic read and write sequence for information storage and retrieval. The H and S arrows indicate stable magnetization directions of the hard and soft films, respectively. A read current pulse results in a field large enough to rotate the soft film magnetization S to a position nearly perpendicular to the easy axis but small enough to rotate the hard film only a few degrees. This rotation of the soft film magnetization induces a voltage in the sense/digit line, which is interrogated as a logic one or zero. When read current is removed, the demagnetizing field of the hard film rotates the soft field

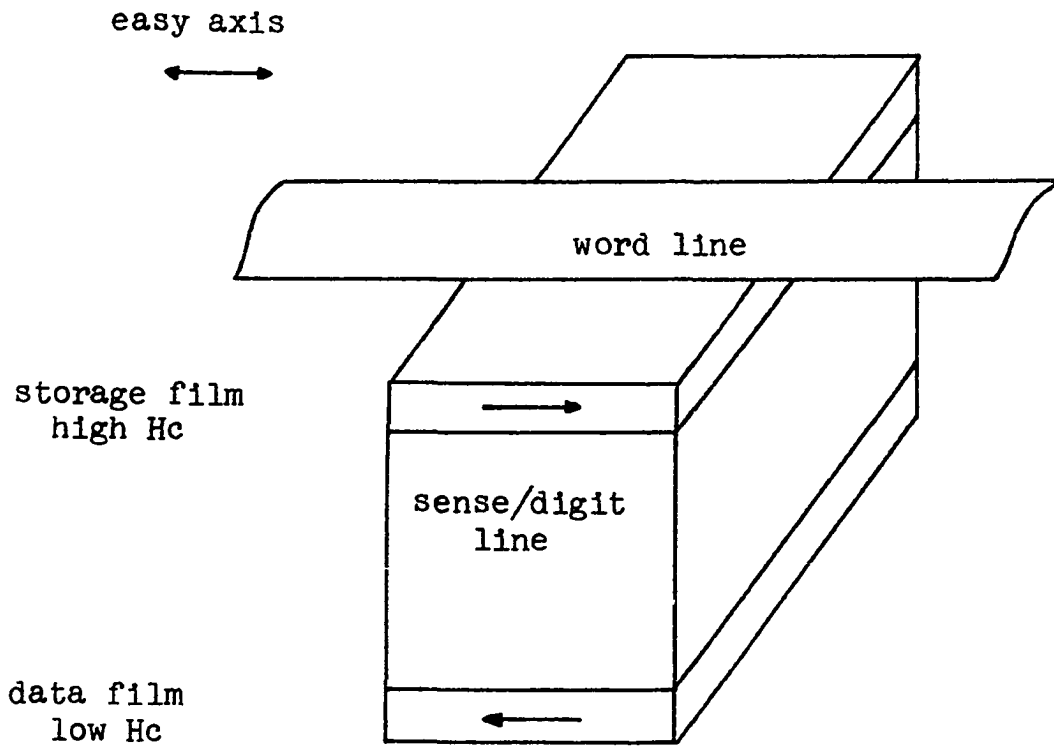


Figure 1. Memory storage element


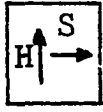

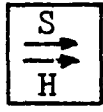
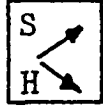
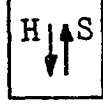

	Magnetizing configuration	Applied field	Operation
Read		None	Bit stored, element ready to be read
		Hread →	Read current on, soft film switches
		None	Soft film reverts to original state
Write		Hwrite →	Write current on, both films switch
		Hwrite Hdigit	Write and digit currents on
		Hdigit ↓	Write current removed, digit current on
		None ↓	Digit current removed, writing complete

Figure 2. Read and write sequence

magnetization back to its original state.

The write operation begins by the application of a write current pulse large enough to rotate both the hard and soft film magnetization by 90° . A digit current pulse is then applied, tipping the magnetizing vectors in opposite directions. Removal of write current allows the digit field to drive the magnetization along the easy axis. Removal of digit current leaves H and S vectors coupled in the easy direction, ready for interrogation.

Fabrication Considerations

Fabrication problems of closed flux, multilayer thin film structures due to problems originating in metal physics have been investigated by Ahn and Freedman.^{15,16} Some of these problems are:

1. The nucleation and growth of each evaporated layer is influenced by the preceding layer;
2. Interfacial diffusion between magnetic films and metal conductors can bring about a change in magnetic properties;
3. Surface roughness and a large grain size of a conductor layer may change magnetic properties.

These problems suggest a tight control of deposition parameters, especially substrate temperature. The lower temperature limit is determined by maximum tolerable skew due to angle of incidence effects, while the upper limit

is primarily due to interfacial diffusion and roughness of the conductor layer resulting from irregular grain growth.

The degradation of magnetic properties of the upper magnetic layer can be reduced by introducing a thin intermediate layer between the Permalloy and copper. Ahn and Freedman have observed a coercive force reduction of nearly two to one when a titanium intermediate layer approximately 400 Å thick is deposited as a metallic intermediate layer, at the Permalloy deposition temperature.^{15,16} They also report that the decrease in coercive force can be made larger, if titanium is deposited at lower temperatures (- 200° C), however such a temperature would prove impractical when producing films in production quantities.

Consideration must also be given to positioning of the data film and storage film. The data film is to have a low coercive force that must be tightly controlled if adequate read current margins are to be obtained, thus it is positioned next to the smooth glass substrate. The storage layer with its higher coercive force can be positioned above the copper layer.

Since magnetostatic coupling of two magnetic layers requires a small separation and since digit line resistivity must be small, especially for long lines, a high conductivity metal is required. Copper is desirable because of its low resistivity, however a silver-copper alloy is better suited.

The higher recrystallization temperature of the alloy permits higher substrate temperatures before surface roughness becomes prohibitive.

Although the major factor influencing the magnetic materials is surface roughness, the effect of diffusion between copper and the Permalloy underlayer is also noticeable. Ahn and Freedman have reported a 10% increase in coercive force of magnetic underlayer due to copper diffusion, when deposition temperatures are 200° C.^{15,16} As reported by Crowther¹⁹ the effective coercive force of Permalloy is raised by copper diffusion, however no significant increase is noted in dispersion.

The low coercive force data film should be fabricated from 82-18 composition nickel-iron because of the near zero magnetostriction and dispersion of this composition. A nickel-iron-cobalt composition is best suited for the magnetically hard storage layer since coercive force and anisotropy field increase with increasing cobalt. A non-magnetostrictive composition has been shown by Bradley,²⁰ to be approximately along a line of constant nickel to iron ratio, as depicted in Figure 3. Lampert²¹ has recently shown anisotropy field to increase nearly linearly with cobalt up to approximately 15%, as shown in Figure 4.

The storage film must have a high anisotropic field to avoid creep when read current is applied. Control

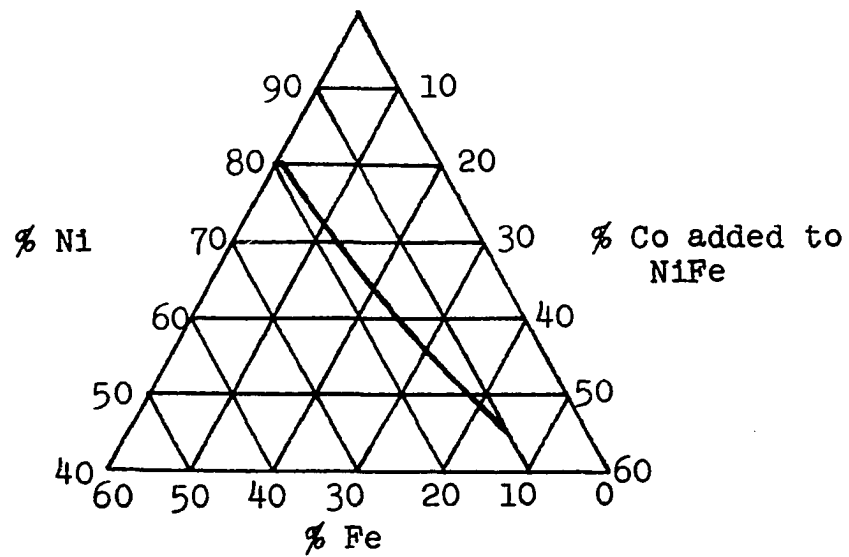


Figure 3. NiFeCo composition having zero magnetostriction

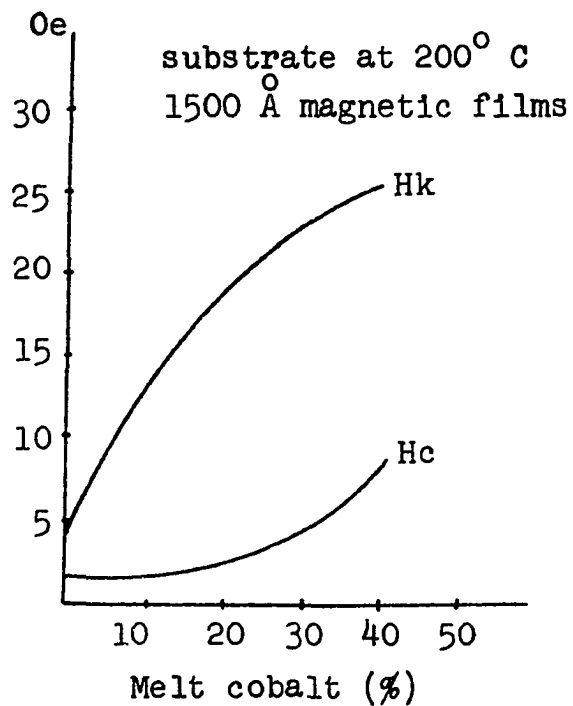


Figure 4. Hc and Hk variation with cobalt

Data⁷ suggests a film containing about 15% cobalt. Such a composition will have a coercive force higher than predicted in Figure 4, because of an irregular copper surface.

EXPERIMENTAL EQUIPMENT AND FABRICATION RESULTS

NDRO Memory Tester

The memory tester, pictured in Figure 5, was built to rapidly determine the read/write curves of each NDRO thin film sample. The memory tester was later modified to the extent that it was capable of supplying control signals to the partially populated test memory.

A sequence of programmable read, write, and digit current pulses are sent to the sample under test. Test sample output signals are directed to differential amplifiers and the differential amplifier output is observed on an oscilloscope. Various tests can be performed on the test sample by controlling both the number of current pulses and their magnitude.

The one foot square tester is completely self contained, except for external power supplies. Located inside the chassis are 150 TTL integrated circuits, 70 transformers and 70 transistors.

Sixty-four eight bit words can be sequentially tested. Sixty-four word lines and eight digit line pairs connect the test sample to the tester. Each word is completely tested, followed by an address sequencer advancing to the next word.

A test cycle consists of five minor cycles. At the end of a test cycle, the address sequencer advances to the next word which is subjected to testing by the five minor

cycles. As depicted in Figure 6 minor cycles are prehistory, write, adjacent disturb, read disturb and read. Prehistory and write are generally used together, prehistory creep writing the test cell until nearly all magnetization is in the same direction and write reversing the magnetization. The adjacent disturb cycle applies word current to word lines adjacent to the word line under test and stores either a logic one or zero in adjacent cells. Read disturb and read test NDRO storage capabilities by repeated application of read current pulses. It is possible to individually disable all but the read cycle through the setting of switches located on the tester panel.

The number of current pulses in four of the minor cycles are variable from 1 to 10^7 , by powers of 10. That is, each minor cycle can have 1, 10, 100, or up to 10^7 current pulses. The adjacent disturb cycle applies word current to word lines adjacent to the line selected by the address sequencer, and contains 2, 20, 200, up to 2×10^7 current pulses. Seven TTL integrated circuit decade counters combine to form a 10^7 decade counter, used in determining the number of current pulses in each minor cycle.

Six amplitude controllable current sources supply read, write, and digit current pulses. The maximum write and digit current sources are enabled for prehistory and adjacent disturb while the minimum write and digit current sources

are enabled for write. The maximum and minimum read current sources are enabled during read disturb and read, respectively.

Eight data switches on the tester panel are used to enter data into test samples. Switches associated with prehistory and adjacent disturb control the setting of digit current in the same or opposite direction from write digit current.

Evaporation Procedure

Experimental NDRO thin film arrays were made by deposition of magnetic and metallic materials by electron beam heating. Depositions were performed in a vacuum of about 2×10^{-5} Torr in the presence of a 50 Oe orientating field. The field was found to vary by approximately ± 5 degrees from the center of the 2 in. x 4 in. substrate holder.

The deposition system was a conventional vacuum system with an 18 inch glass bell jar. A rotatable table was used to hold all deposition materials so evaporation could be performed with a single electron beam in a single pump down. A quartz crystal was used to determine evaporation rates and monitor thickness. A current meter in the electron beam gun high voltage power supply was also used to control evaporation rates.

Substrates were placed 13 inches directly above the source to reduce angle of incidence effects. Flux density

of film samples varied by less than 5% over the surface of the substrate holder while coercive force for a single layer 1500 Å film typically varied by 10%.

All materials except those containing Permalloy were evaporated in tantalum crucibles. Permalloy was evaporated in carbon cloth, graphite and alumina crucibles with alumina giving the best results. After several evaporations in the alumina crucibles, a layer of slag was found to form over the Permalloy, with a resulting increase in coercive force which became more pronounced when thicker films were evaporated. To eliminate this problem a new 3.5 gram Permalloy slug was placed in a new alumina crucible before each evaporation.

Deposition was performed through a wire mask onto heated glass substrates. Heating of glass substrates not only improved film characteristics but also increased adhesion between glass and film. Wire masks were made on a lathe by winding nichrome wire under tension onto a nonmagnetic stainless steel frame. The thermal expansion coefficients of nichrome wire and stainless steel proved to be matched closely enough such that the wires did not lose tension after repeated temperature cycling. A brass block was placed on top of the glass substrate during deposition to hold the substrate in place and to distribute heat over the substrate. Temperature was monitored with a standard

thermocouple, placed on a glass substrate and positioned in the substrate holder.

A glass substrate was placed in the substrate holder such that it was not masked. This continuous film sample was used for hysteresis loop testing.

Test samples were deposited on No. 2, 22 millimeter square, Corning Cover Glass. Substrates were scrubbed and cleaned ultrasonically in an Alconox solution, rinsed ultrasonically in distilled water followed by a vapor degreasing and then stored in the degreaser until ready for use.

Array Fabrication

Test samples were made by evaporation through a wire mask wound from 3.1 mil nichrome wire. Film strips tested were 3.8, 5.8, and 7.8 mils wide, with 3.1 mils separating each strip. Some nonuniformities in the wire mask were encountered, therefore film samples were selected to give the proper width.

Figure 7 depicts a typical cross section of the NDRO storage device. A $100 \overset{\circ}{\text{A}}$ layer of chromium is vacuum deposited to increase adhesion between the glass substrate and first Permalloy layer. Sequential deposition of a low coercive force data film, a metallic layer of 10% silver, 90% copper, a $400 \overset{\circ}{\text{A}}$ titanium smoothing layer and a high coercive force storage film, through the wire mask, forms

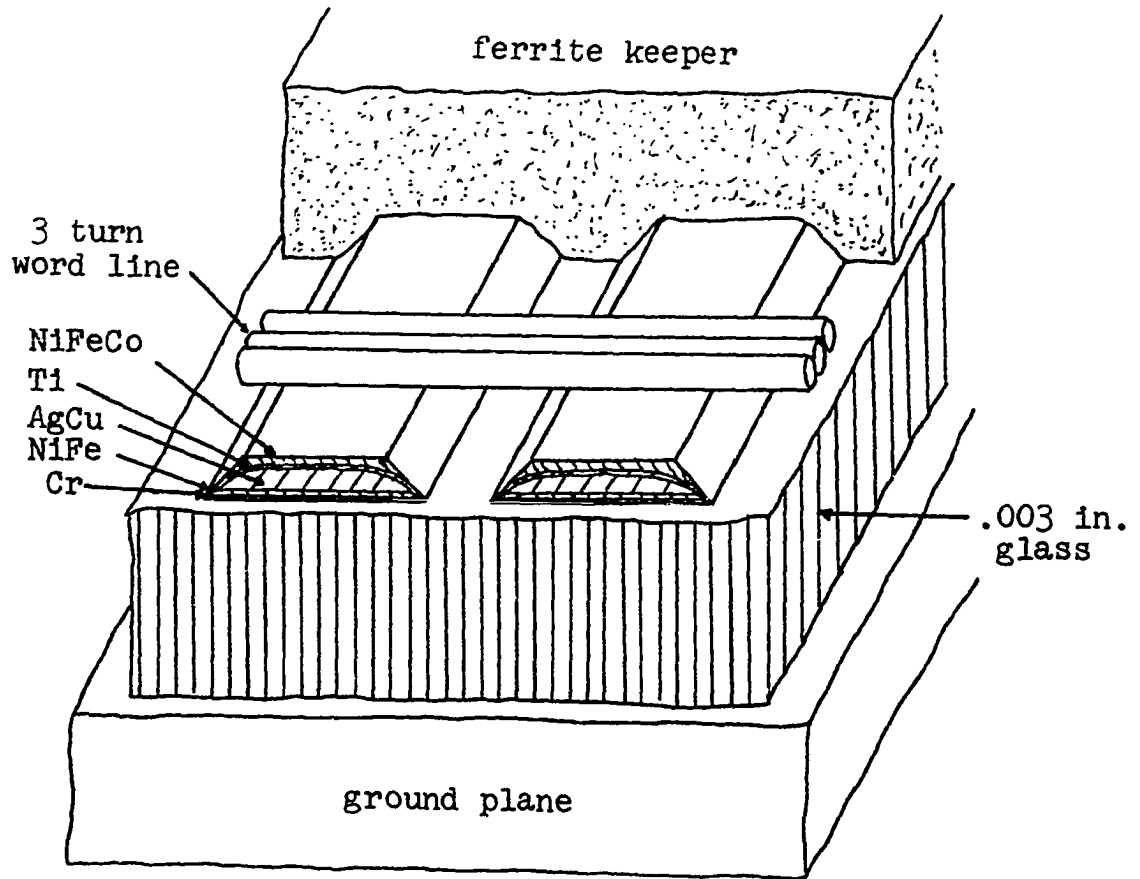


Figure 7. NDRO storage element

continuous film strips closed in the easy direction. The deposition conditions of the film structure and cross sectional dimensions considered are summarized in Figure 8.

Film samples were placed on a small brass ground plane, for testing purposes. As depicted in Figure 9, three turns of 2.4 mil wire form 8 mil word straps, wound on 16 mil centers. Smaller word lines were not used since the higher resistance would limit word current amplitude supplied by the memory tester, to values lower than desirable.

The concept of multiturn windings as shown in Figure 9 is a method of improving the efficiency of thin film memory elements and was first introduced by Pohm.⁴ Another feature shown in Figure 9 is a ferrite powder keeper covering the memory array. This material not only reduces word current but also increases adjacent bit disturb margins by reducing bit to bit word field coupling.²²

Film strips are shown connected in a hairpin configuration for attachment to a differential sense amplifier. In this arrangement read current, coupled to each film strip is cancelled as common mode noise at the sense amplifier. Another advantage of this configuration is an increased output signal. Since two film strips are employed, each stored bit of information contains two storage cells. Sense/digit wires were soldered directly to the film strips. Little trouble was encountered, when appropriate soldering

Composition	Layer thickness (Å)	Substrate temperature (°C)	Evaporation rate (Å/sec)
Cr	100	25-250	10
NiFe	1K-3K	25-250	30
AgCu	1K-20K	25-250	30-40
Ti	400	25-250	15
NiFeCo	1K-3K	25-250	30

Figure 8. Deposition conditions

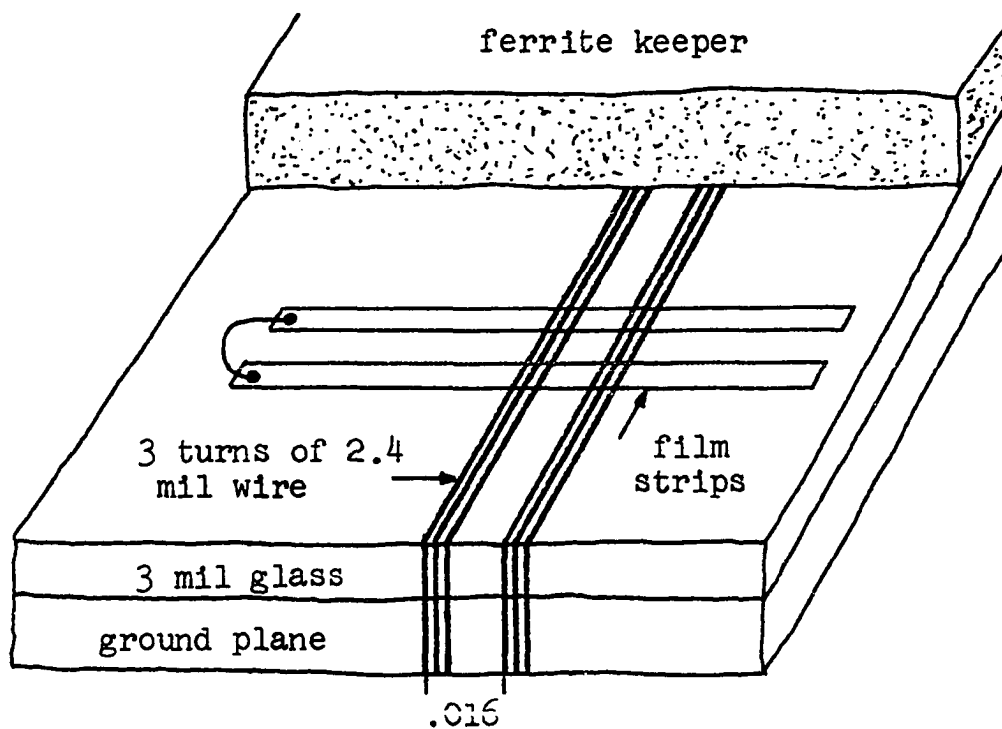


Figure 9. Test sample wiring configuration

techniques were used.

Figure 10 illustrates read, write, self disturb and adjacent disturb curves for a test sample with storage film having 10% cobalt doping. Its properties are depicted in Figure 11.

Figure 10A shows a plot of single pulse digit current versus word current to write to 80% magnetization. Writing was accomplished by creep writing at least 10^4 times with high currents to establish a magnetic prehistory and then single writing with digit current polarity reversed. Curves for 3.8, 5.8, and 7.8 mil film strips are depicted. Note that, as the strip narrows writing becomes easier since digit field is inversely proportional to film width.

Figure 10B illustrates film output as read current amplitude varies and read current rise time remains constant at 40 nsec \pm 10%. A test cell was first written as explained above, and then read at least 10^5 times before recording output signal. The curves are seen to rise to a maximum amplitude and then decreases as the storage film is disturbed.

Figure 10C depicts self disturb data obtained by writing once during the prehistory cycle, creep writing with digit polarity reversed at least 10^4 times during write cycle and then noting sense signal after at least 10^4 reads, with read current set 10 mA below peak value. The curve

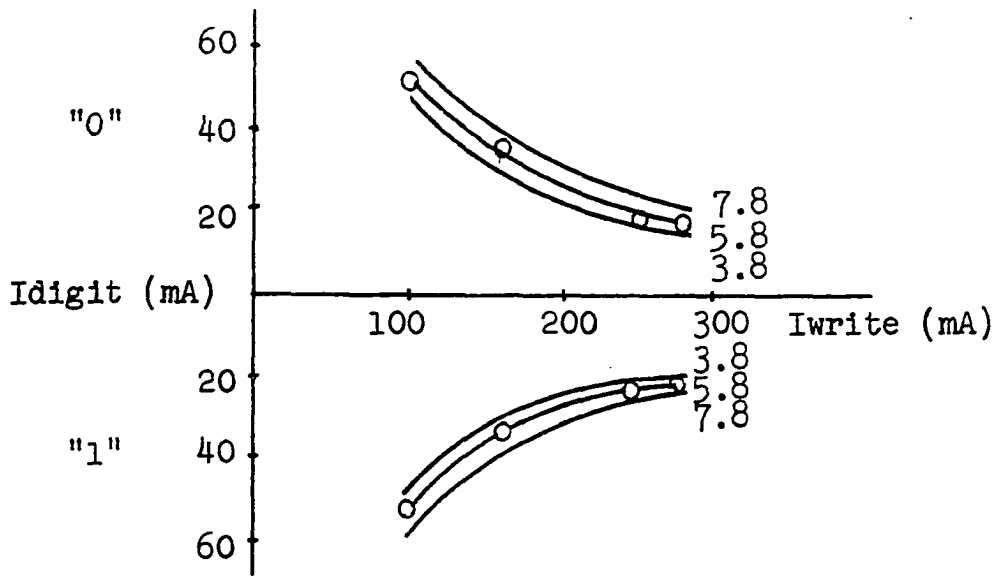


Figure 10A. Write curve for 10% cobalt doped storage film

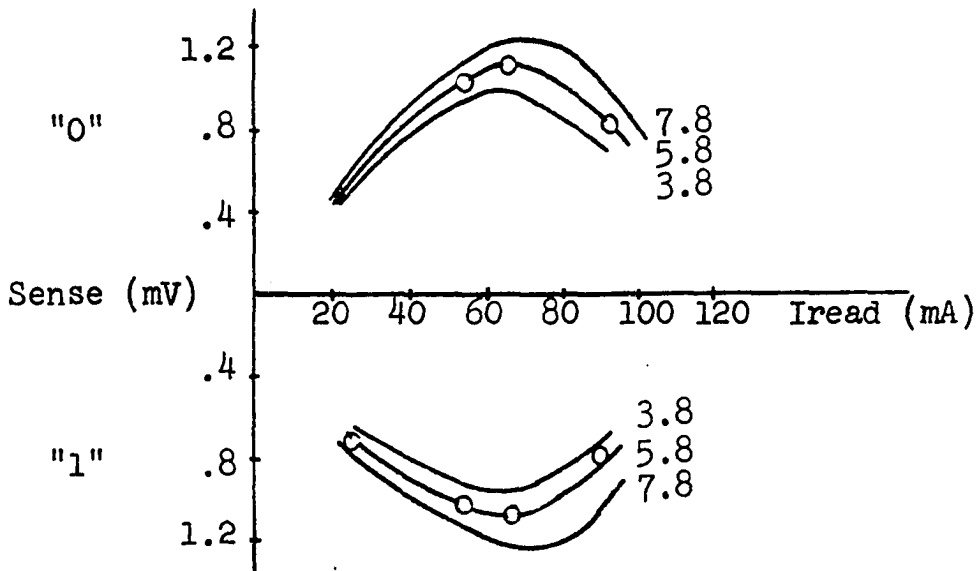


Figure 10B. Read curve for 10% cobalt doped storage film

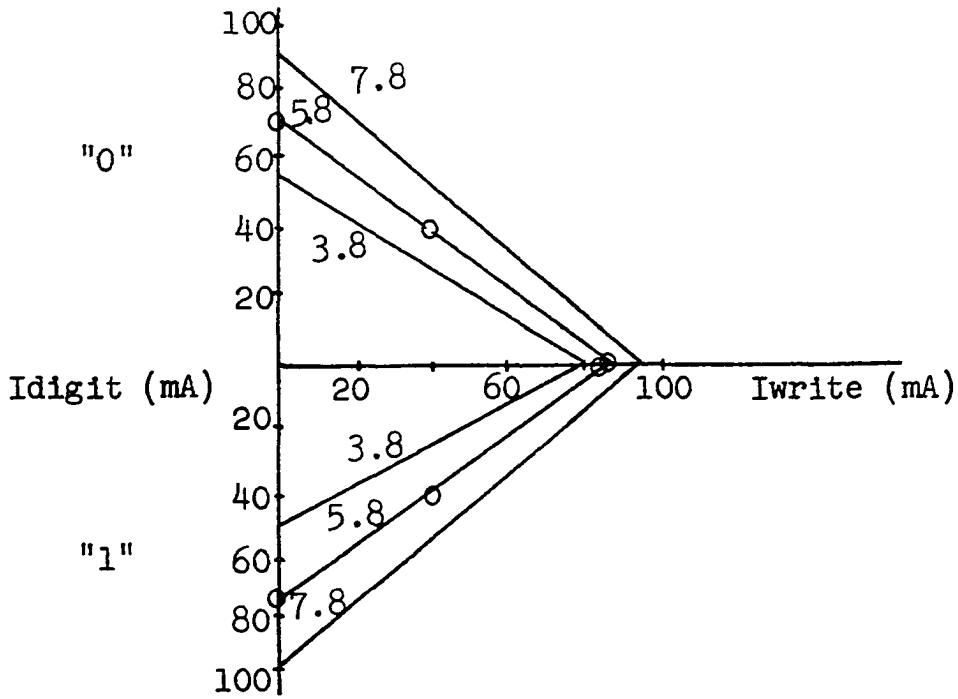


Figure 10C. Self disturb curves for 10% cobalt doped storage film

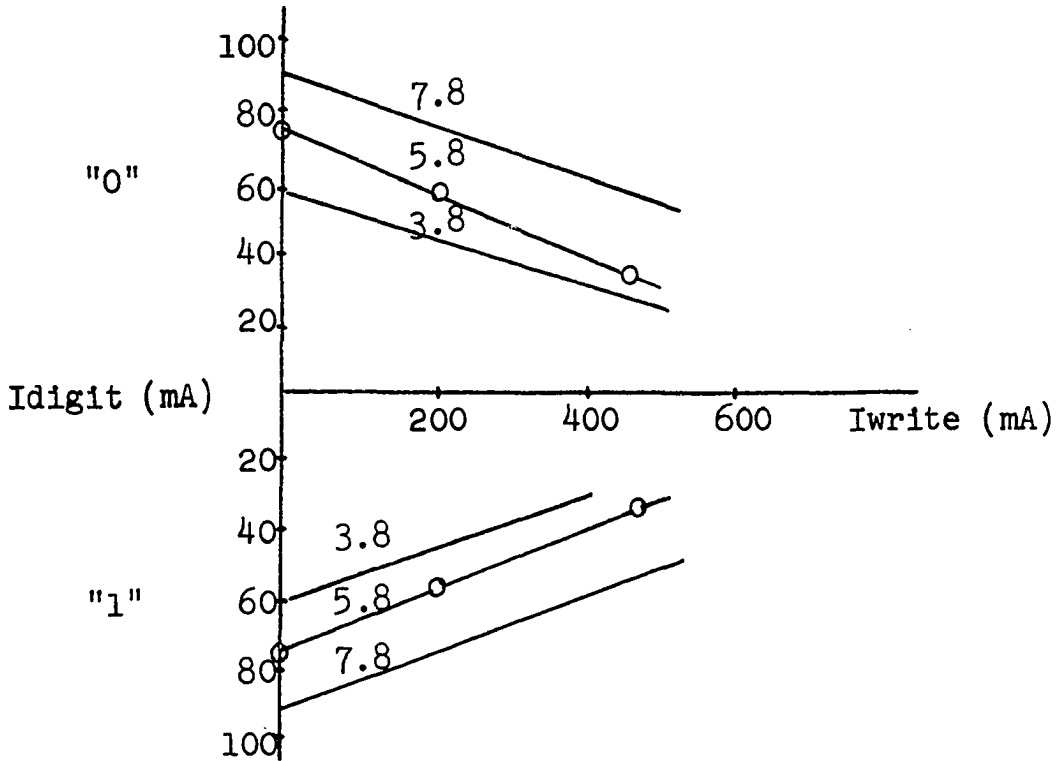


Figure 10D. Adjacent disturb curves for 10% cobalt doped storage film

represents write current versus digit current necessary to reduce sense signal by 20% from that value obtained when the write cycle is disabled. Note that the 3.8 mil strip intersects the vertical axis at a lower point than the wider strips, indicating a lower digit current disturb threshold.

As the relative width of the film is decreased the coercive force decreases due to an increasing demagnetizing field,²³ since the films are not perfectly coupled. The lower coercive force will result in lower creep margins, as depicted in Figure 10C.

Adjacent disturb curves, shown in Figure 10D were obtained by sequentially:

1. Establishing a magnetic prehistory and then writing;
2. Disturbing adjacent lines at least 10^4 times through the adjacent disturb cycle;
3. Noting signal output after at least 10^4 reads.

The adjacent disturb curve represents adjacent word current versus digit current when sense signal is reduced by 30%.

Adjacent disturb curves and self disturb curves intersect the vertical axis at identical points, as expected. Note that the smaller strip is more sensitive to adjacent word fields, because of its lower digit disturb threshold.

Holding substrate temperature constant during evaporation proved to be a problem. As shown in Figure 11 initial

Composition	Layer thickness (Å)	Substrate temperature (°C)	Magnetic properties (Oe)
Cr	100	180	
82-18 NiFe + .75% Fe	1,500	180-175	Hc = 2.5, Hk = 5
90-10 CuAg	10,000	180-160	
Ti	400	180	
82-18 NiFe + 10% Co	1,500	180-175	Hc = 13, Hk = 14

Figure 11. Deposition conditions and magnetic characteristics for a 1500 Å test sample with 10% cobalt doped storage film

substrate temperature was 180° C, however once the shutter was opened, temperature began to drop and reached a low of 160° C during copper evaporation.

Tiny balls of molten copper were found to splatter onto the surface, producing irregularities in film strips. Reduction of the copper evaporation rate eliminated this problem.

Initial 1500 \AA magnetically soft data films had a coercive force of 5 Oe to 10 Oe, and proved to be nickel rich when subjected to a magnetostrictive test. Coercive force was reduced to 2.0 Oe to 3.5 Oe by adding an additional .75% iron to the 82-18 Ni-Fe composition. These films were only slightly magnetostrictive, with excess iron indicated.

Tests were performed on adjacent film strips to determine whether neighboring fields reduced film operating margins. No adjacent digit field disturb problems were noticed. No attempt was made to reduce film spacing below 3.1 mils since materials were not readily available to construct such a mask.

The thickness of both films depicted in Figure 11 was about 1500 \AA . Films differing in thickness by several hundred angstroms were evaporated however it can not be reported that an improvement of read/write curves was observed. Read/write currents and hysteresis loop measurements were accurate to about $\pm 10\%$. If accuracy were improved to $\pm 1\%$, then an improvement would probably be

noted, if film thickness were adjusted to improve magnetic coupling such that magnetic flux of both films was equal.

It was observed that output signal could be increased by increasing the percentage of cobalt doping. A film was fabricated with the same properties as those depicted in Figure 11, with the exception of the storage film whose coercive force and anisotropic field are 12 Oe and 20 Oe respectively and whose zero magnetostrictive composition is 84-16 Ni-Fe plus an additional 20% cobalt. The read and write curves of this film are shown in Figure 12. It should be noted that sense signal is greater since creep threshold has increased by approximately 20 mA. The write curve shows that the storage film is now harder to write, however write currents are still within acceptable limits.

The increase in output signal can be attributed to an increased anisotropic field of the storage film, allowing higher read currents before stored information is destroyed. Samples with a greater percentage of cobalt doping were tried, however an increase in sense signal was not observed. Samples with 15% cobalt doping exhibited less signal, therefore it was concluded that 20% cobalt doping was near optimum.

Digit disturb margins were increased by raising coercive force of the storage film. Figure 13A depicts how digit disturb current is influenced by coercive force

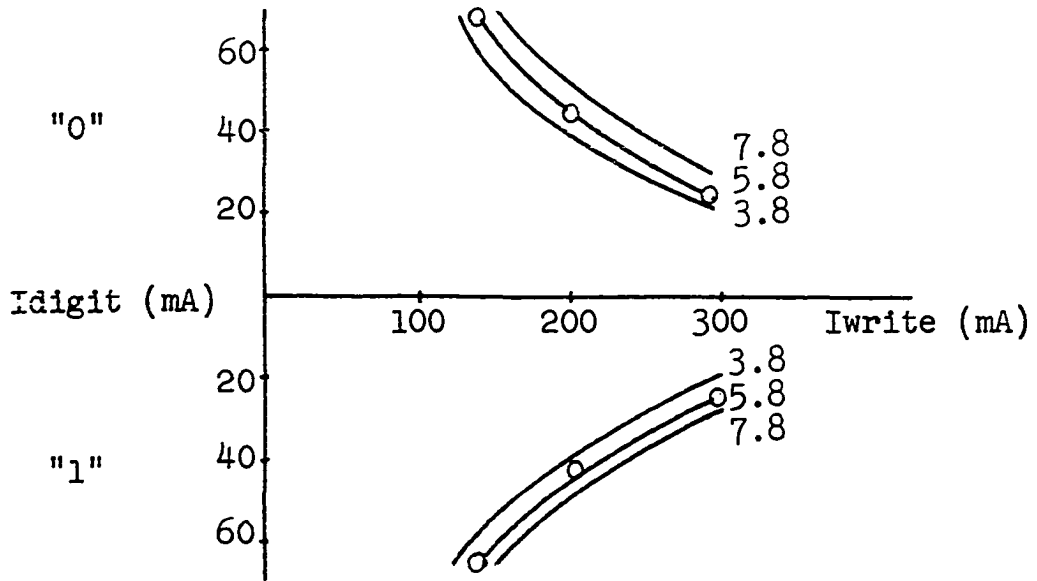


Figure 12A. Write curves for 20% cobalt doped storage film

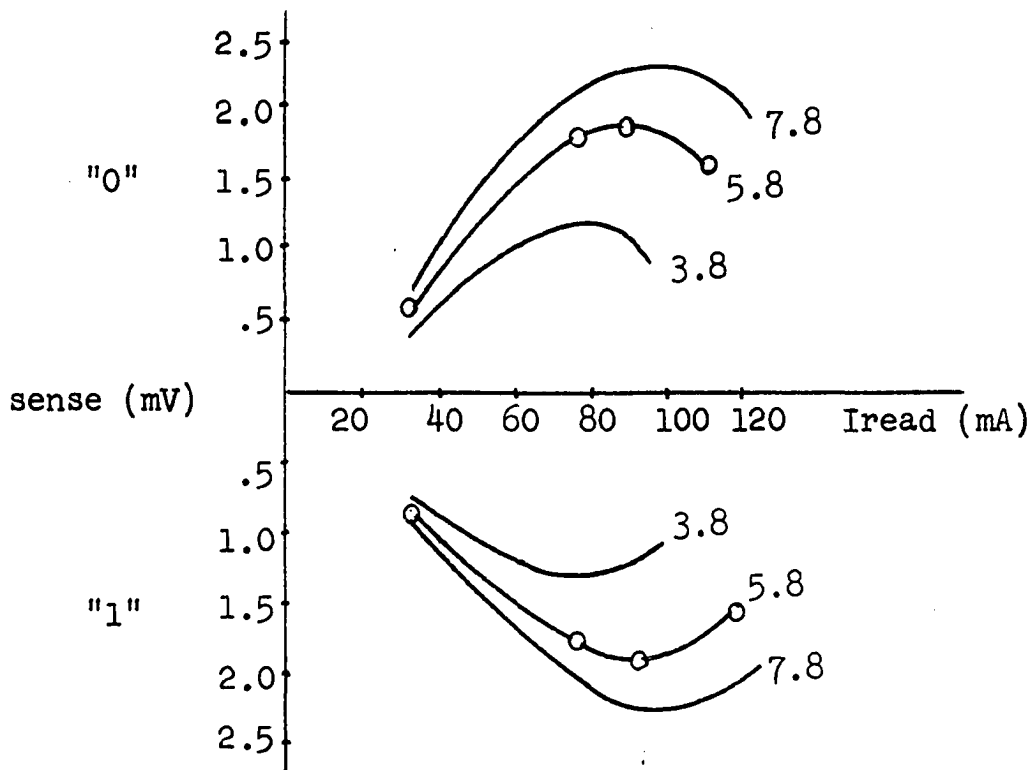


Figure 12B. Read curves for 20% cobalt doped storage film

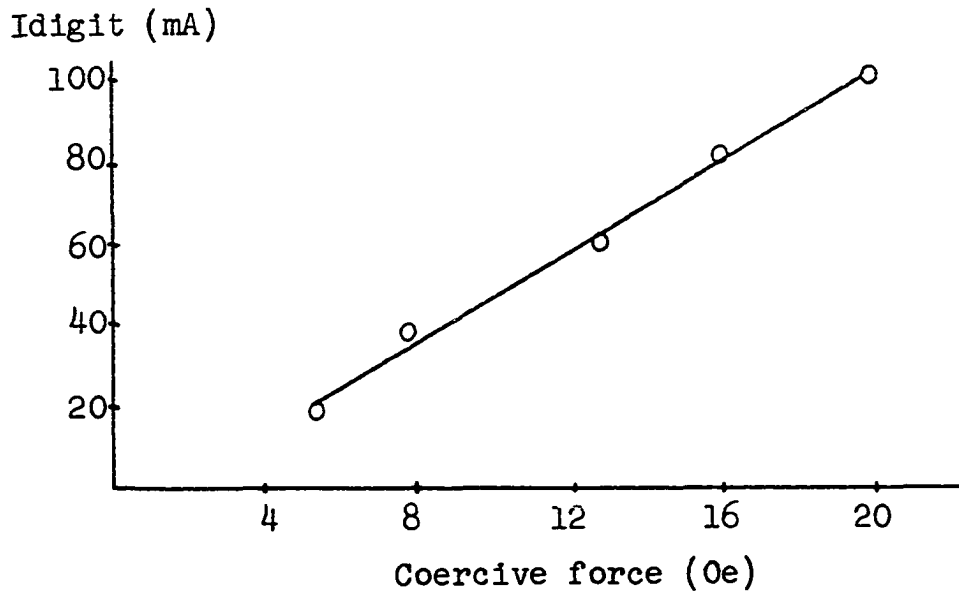


Figure 13A. Self disturb digit current versus coercive force for 1500 Å multilayer 5.8 mil film with 15% cobalt doped storage film

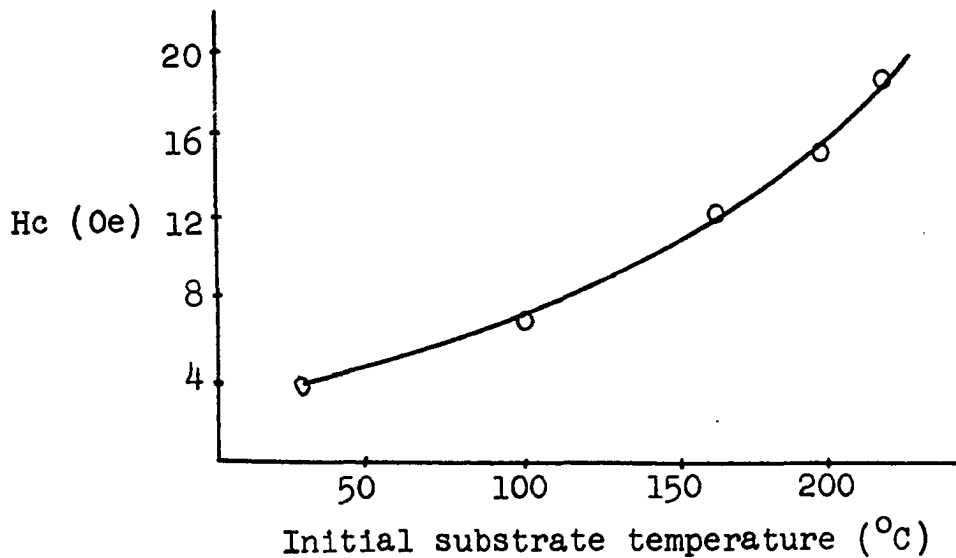


Figure 13B. Typical variation of Hc with temperature for multilayer film with 1.5 KÅ magnetic layer and 10 KÅ metallic layer

and Figure 13B illustrates the temperature dependence of coercive force. Crowther has shown a strong correlation between dispersion and coercive force in cobalt films, therefore coercive force should be low enough to reduce dispersion yet high enough to establish adequate disturb margins. Fortunately, cobalt doped films exhibit low dispersion,²¹ therefore a higher coercive force can be tolerated before dispersion becomes noticeable.

Figure 14 illustrates read, write, adjacent disturb and self disturb curves for a test sample having 20% cobalt doping and a storage film coercive force of 20 Oe. Figure 15 summarizes the properties of this sample. Note that peak output signal for the 5.8 mil film is 2 mV at 90 mA while write and digit current are 200 mA and 45 mA respectively. Figure 16 depicts sense signal variation versus digit current for the 5.8 mil film sample. Little shifting of write curves can be seen due to effects of skew and dispersion.

Hysteresis loops of the continuous film test sample and mechanically defined film strip sample for 60 cycle longitudinal drive are shown in Figures 17 and 18 respectively. The inner easy axis hysteresis loop of Figure 17A shows the magnetically soft information film while the outer loop shows the dual nature of the film. Figure 17B depicts the hard axis hysteresis loop. Demagnetizing effects due to film strips are shown in the hysteresis loops of Figure 18.

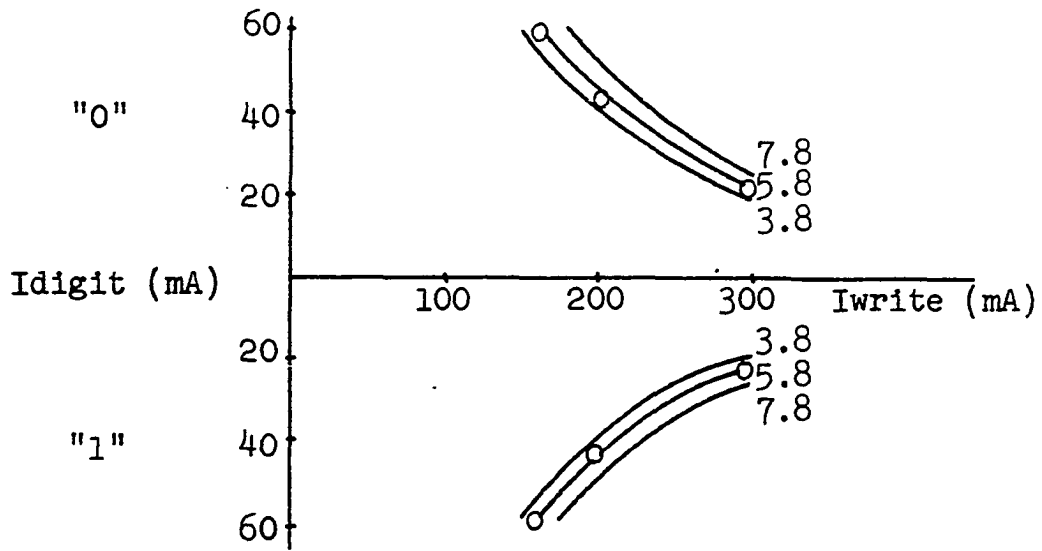


Figure 14A. Write curves for test sample with 20% cobalt doped storage film and H_c of 20 Oe

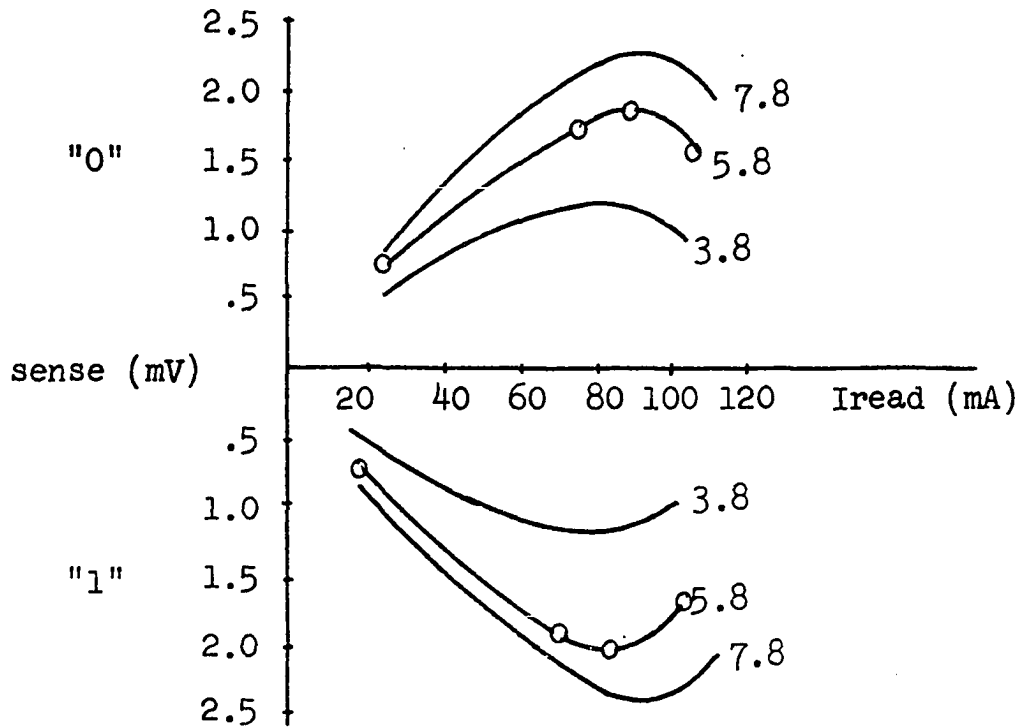


Figure 14B. Read curves for test sample with 20% cobalt doped storage film and H_c of 20 Oe

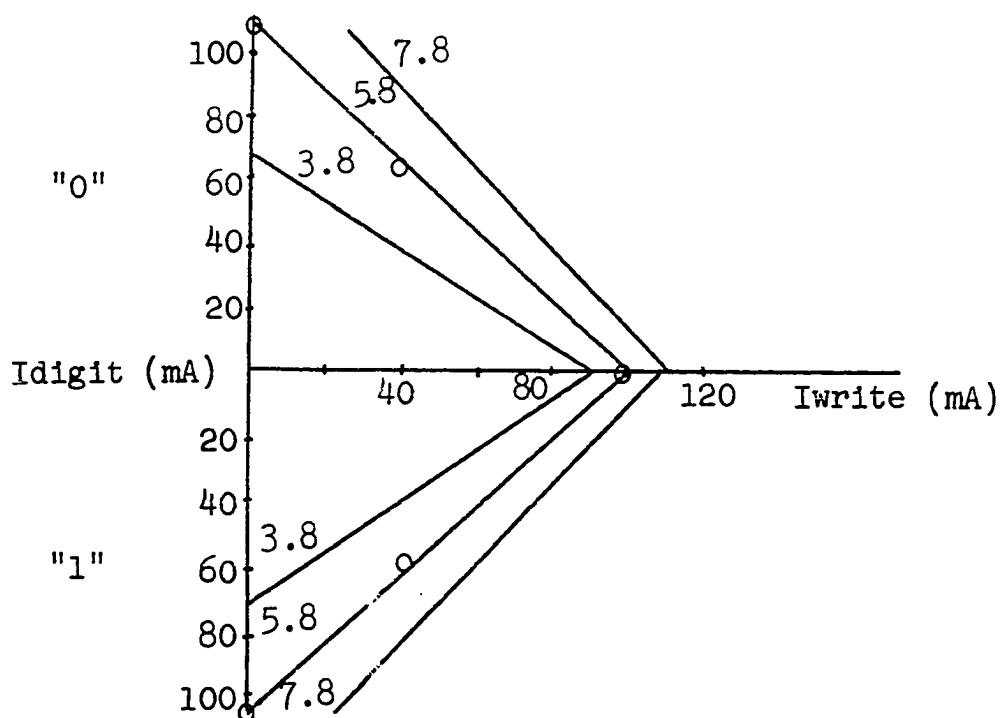


Figure 14C. Self disturb curves for test sample with 20% cobalt doped storage film and H_c of 20 Oe

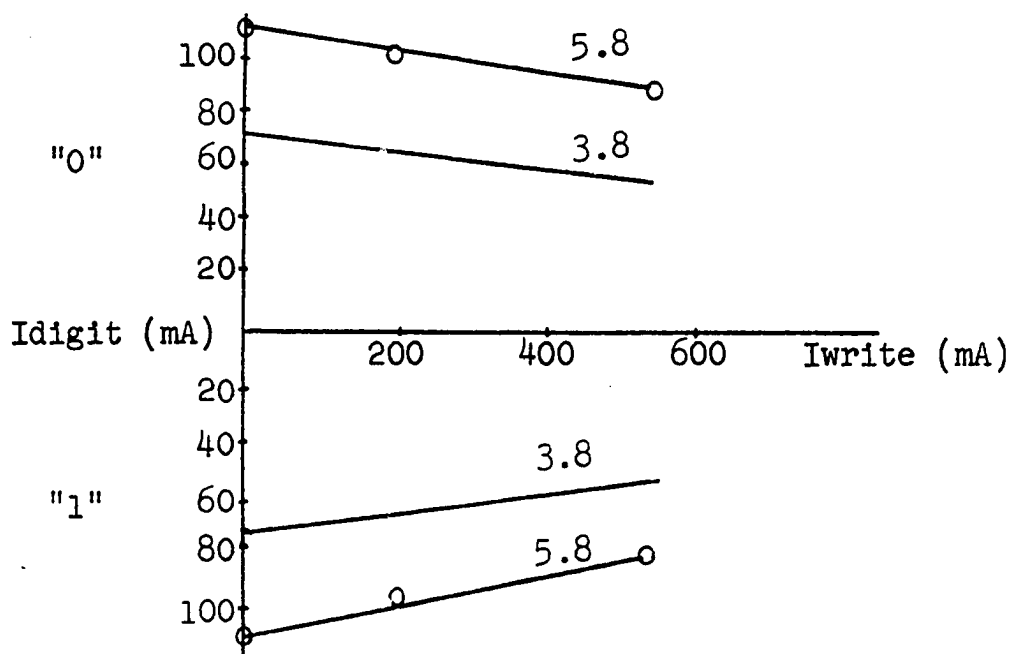


Figure 14D. Adjacent disturb curves for test sample with 20% cobalt doped storage film and H_c of 20 Oe

Composition	Layer thickness (Å)	Substrate temperature (°C)	Magnetic properties (Oe)
Cr	100	230	
82-18 NiFe + .75% Fe	1,500	230-225	Hc = 2, Hk = 5.5
90-10 CuAg	20,000	225-200	
Ti	400	225	
84-16 NiFe + 20% Co	1,500	225-220	Hc = 20, Hk = 21

Figure 15. Deposition conditions and magnetic characteristics for a 1500 Å test sample with 20% cobalt doped storage film and coercive force of 20 Oe

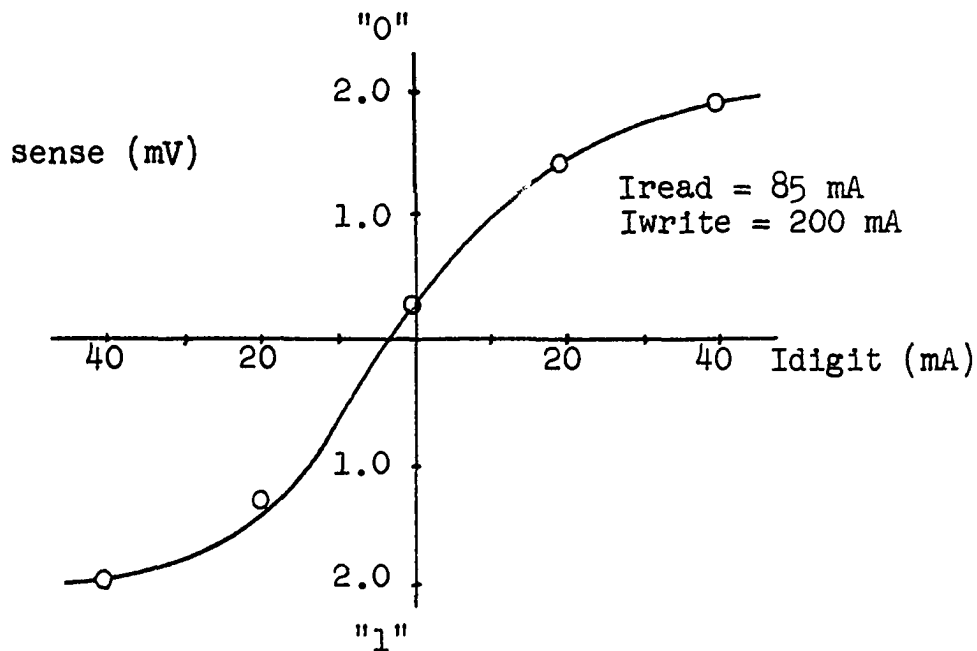
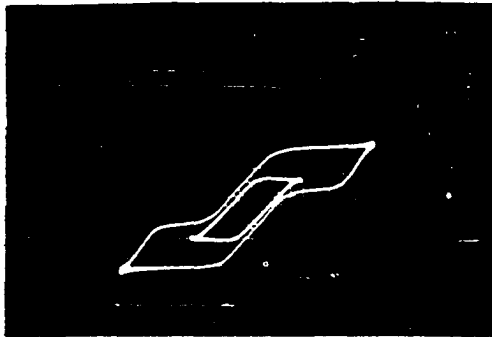
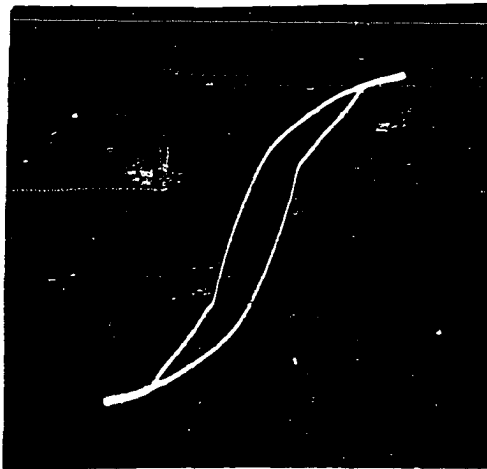
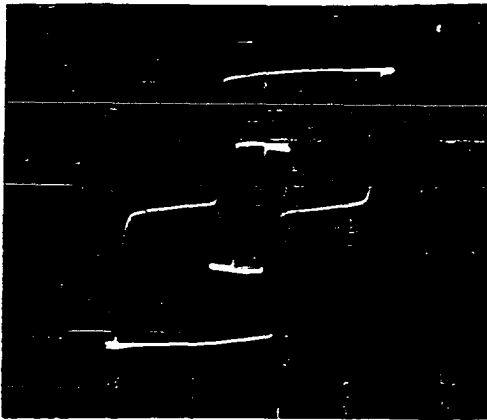


Figure 16. Output signal versus digit current for 5.8 mil test sample with 20% cobalt doped storage film and Hc of 20 Oe

Figure 17A. Easy axis hysteresis loops of continuous film test sample depicted in Figure 15; inner loop shows data film and outer loop combined films; horizontal scale, 12 Oe/division

Figure 17B. Hard axis hysteresis loop of continuous film test sample depicted in Figure 15; horizontal scale, 12 Oe/division

Figure 18. Easy axis hysteresis loops, of film depicted in Figure 15 with mechanically defined film strips, demonstrate demagnetizing fields; horizontal scale, 12 Oe/division



The film sample depicted in Figure 11 had a $10 \text{ K}\overset{\circ}{\text{A}}$ metallic layer while the sample depicted in Figure 15 had a $20 \text{ K}\overset{\circ}{\text{A}}$ metallic layer. Metallic layers ranging in thickness from $2 \text{ K}\overset{\circ}{\text{A}}$ to $20 \text{ K}\overset{\circ}{\text{A}}$ were evaporated, with no apparent change in magnetic flux coupling properties being noted. The upper limit on metallic layer thickness which was $20 \text{ K}\overset{\circ}{\text{A}}$, was due to limits imposed by the vacuum system, namely a crystal failure and peeling of copper from the bell jar.

Since the magnetic films are closely coupled it would be expected that $2 \text{ K}\overset{\circ}{\text{A}}$ to $3 \text{ K}\overset{\circ}{\text{A}}$ films could be fabricated without excessive demagnetizing fields, the thicker films being more desirable because of increased output signal. Coupled films having magnetic layers ranging in thickness from $1 \text{ K}\overset{\circ}{\text{A}}$ to $3 \text{ K}\overset{\circ}{\text{A}}$ were fabricated. Signal output from $2 \text{ K}\overset{\circ}{\text{A}}$ films was 20% to 25% greater than 1500 \AA films, while write currents were nearly the same. To produce a low coercive force $2 \text{ K}\overset{\circ}{\text{A}}$ information film 1.5% iron was added to 82-18 Permalloy, making this film more magnetostrictive than previous samples discussed.

The $2 \text{ K}\overset{\circ}{\text{A}}$ films proved harder to make than the $1.5 \text{ K}\overset{\circ}{\text{A}}$ films. Approximately 95% of the $1.5 \text{ K}\overset{\circ}{\text{A}}$ films were usable, while only about 50% of the $2 \text{ K}\overset{\circ}{\text{A}}$ films were acceptable. The unacceptable films usually had a high information film coercive force. With a better deposition system, it is felt that $2 \text{ K}\overset{\circ}{\text{A}}$ films could be made without much difficulty.

Several 3 KÅ^o coupled films were fabricated by adding 3.3% iron to Permalloy to reduce coercive force. These films were very magnetostrictive and proved extremely difficult to write. Because of the difficulties encountered, an attempt to produce a usable 3 KÅ^o coupled film was not pursued.

LARGE MEMORY DESIGN

Introduction

A partially populated NDRO memory plane representing 10^6 bits was constructed to demonstrate that developed NDRO storage elements can be used in a bulk store memory. Techniques presented can be applied to the design of a memory containing at least 10^7 bits.

Memory Array

Experimental NDRO film arrays were constructed using techniques developed in the fabrication of 5.8 mil test films depicted in Figures 14, 15, and 16. Films 5.8 mils wide were deposited onto 3 mil x 3.6 in. x 1.76 in. glass substrates, through a wire mask wound from 3.1 mil nichrome wire on 8.9 mil centers, with the easy axis parallel to the 1.76 in. side. Characteristics of the film arrays tested in the partially populated test plane are summarized in Figure 19.

The selection of a 5.8 mil wide film proved to be the best compromise between performance and bit density. A 3.8 mil film would increase bit density however higher digit disturb margins, larger output signal and lower sense/digit line resistance are obtainable with the wider film. Sense/digit line wire termination is also simplified because of increased soldering area.

Composition	Layer thickness (Å)	Substrate temperature (°C)	Magnetic properties (Oe)
Cr	100	210	
82-18 NiFe + .75% Fe	1,500	210-205	Hc = 2.5-3 Hk = 5-5.5
10-90 AgCu	20,000	210-185	
Ti	400	210	
84-16 NiFe + 20% Co	1,500	210-205	Hc = 15-16 Hk = 22-23

Figure 19. Characteristics of memory arrays tested in a partially populated memory plane

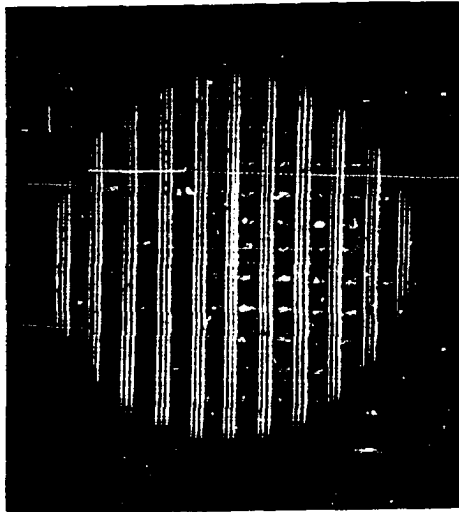


Figure 20. Memory array showing 3 turn word lines on 10 mil centers and 5.8 mil film strip on 8.9 mil centers

Several hundred angstroms of evaporation material was deposited between film strips and produced shorts between adjacent films. Adding weight to force glass substrates nearer the wire mask reduced material thickness, however 50 ohms was still measured between certain strips. Unwanted material was removed and resistance between adjacent strips raised to between 50 Kohms and 100 Kohms by subjecting glass arrays to a weak ferrous chloride etch. The etching process did not produce a noticeable change in magnetic properties of either magnetic film layer.

Tolerance of film samples to adjacent disturb currents was noted during earlier tests and was the determining factor in selecting word line spacing. Three turn word lines were wound from 1.6 mil insulated wire on 10 mil centers and then covered with a ferrite powder keeper. A portion of the memory array without ferrite keeper is shown in Figure 20.

Sense lines were connected in a hairpin configuration to increase signal output and reduce common mode noise. Average measured sense line resistance was 5.7Ω and calculated resistance 5.3Ω . Each array contributes 11.4Ω to sense resistance or approximately $31 \text{ m}\Omega/\text{bit}$. Propagation delay of one film strip was 1 nsec and characteristic impedance approximately 50Ω . Each memory array has approximately 360 word lines and 196 sense/digit film

strips. Since two elements are used per bit, each array represents approximately 36 K bits.

Design Considerations

The problem of memory design is generally one requiring a compromise between system performance and cost. There are many determining factors that influence memory design. There are physical constraints such as line inductance, attenuation and propagation delay which can place an upper bound on system dimensions. There are physical specifications such as size, weight and power consumption which sometimes are determining factors in a given design. There is also an economic constraint which is almost always a determining factor.

One of the prime considerations in the design of any memory system is selection circuitry cost. It has been shown for a linear select memory that array geometry can be arranged to minimize cost.^{7,23} Consider a memory array comprising B bits of storage, organized into N words of M bits each. Assuming that word selection cost w and digit and sense cost s are linear with N and M respectively, the number of words N and bits M to minimize cost should be given by the following expressions:

$$N = \sqrt{B (s/w)} \quad ; \quad M = \sqrt{B (w/s)} \quad .$$

The assumption of linearity of selection cost with N for

large values of N has been shown to be quite good.³ If each sense line is connected to a differential preamplifier, with a gating method which permits several preamplifiers to feed a single amplifier sense cost S becomes the cost of digit drivers and differential preamplifiers.³

To see how physical constraints and economic considerations affect memory organization consider the design of a 10^7 bit memory using high density multilayer arrays. Assume a sense to word cost ratio of 10:1. Organizing to minimize cost yields 10K words, each 1k bits long. Each sense line has a delay of approximately 56 nsec and a resistance of 310 Ω . If read rise time is 30 nsec, sense signal is reduced nearly 50% due to propagation delay alone. Line resistance will further reduce sense signal and make digit drive design difficult. Fortunately other design alternatives exist. Suppose the memory is organized as ten, 10^6 modules, each module being organized to minimize cost. Then each module would have approximately 3.16 K words 316 bits long and sense line delay and resistance of 16 nsec and 100 Ω respectively. Figure 21 depicts the organization of a 10^7 bit memory into ten modules. Note that each sense line connects to a digit driver and sense preamplifier. Additional sense preamplifiers could be added to reduce the number of bits per word.

The problem of connections to sense/digit lines

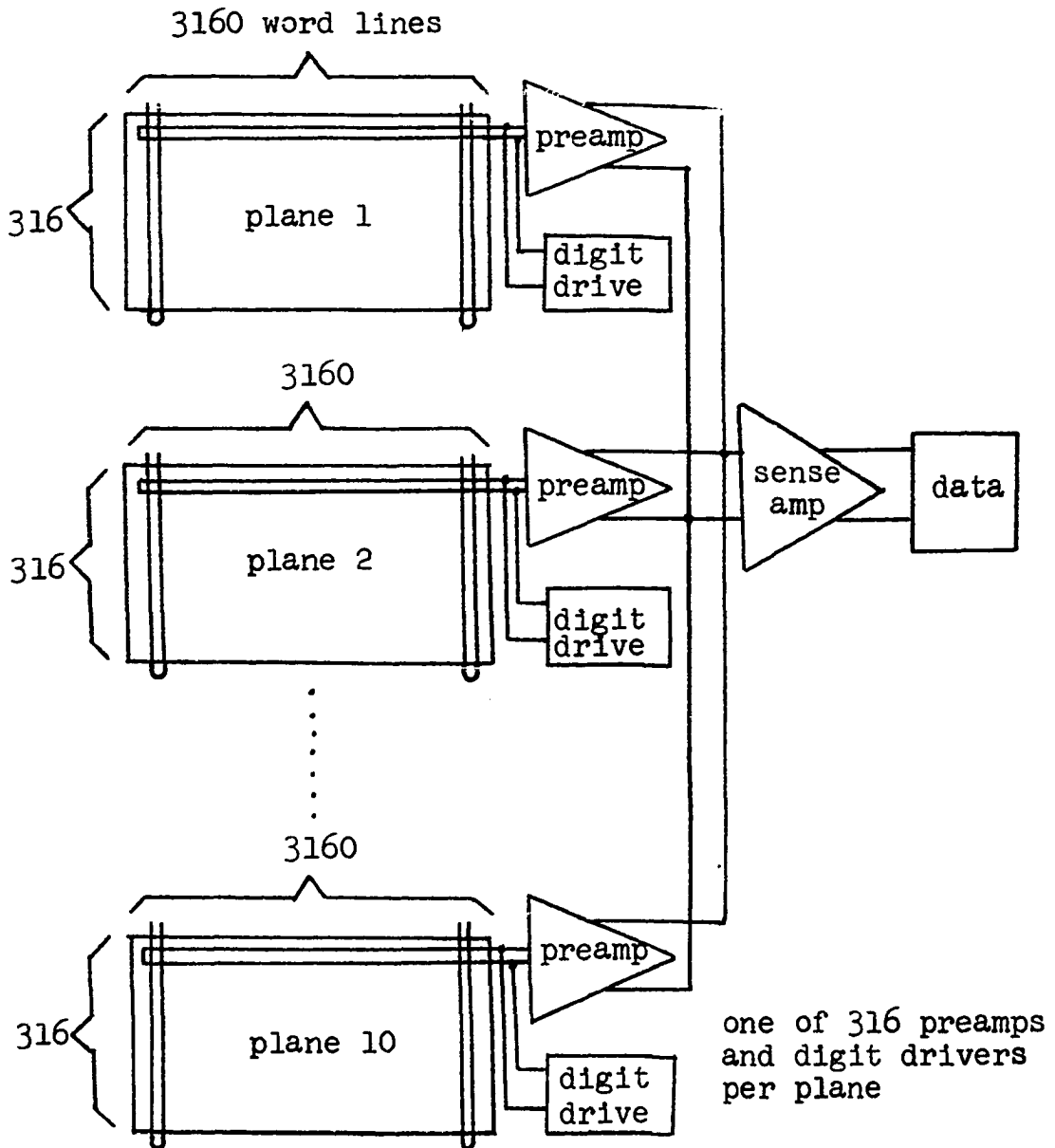


Figure 21. 10^7 bit memory using high density NDRO memory array

represents an important design consideration. In test systems, connections were made by soldering wires individually. For large memory fabrication, solder reflow using infra-red techniques could be adapted.

Test System

The memory test system depicted in Figure 22 was used to evaluate the performance of NDRO storage elements in a large memory plane. The test system is divided into three parts: the tester, control circuitry, and memory arrays. Control signals, six address bits and eight data bits are sent to control circuitry from the tester. Five address bits select one of 32 word lines and one address bit selects sense line preamplifiers.

The memory tester was designed with a 6 usec read or write cycle time. The test plane was cycled at rates up to 300 nsec by first disabling the memory tester and by then using the control circuitry to cycle the test plane on a single address.

The test plane containing memory arrays is divided into four smaller brass ground planes. Each plane contains two memory arrays, however eight arrays can be placed on an individual plane with four arrays per side. Test cells were located at the input ends of sense/digit and word lines, where selection noise is expected to be the greatest. Thirty-two word lines were wound on each of two

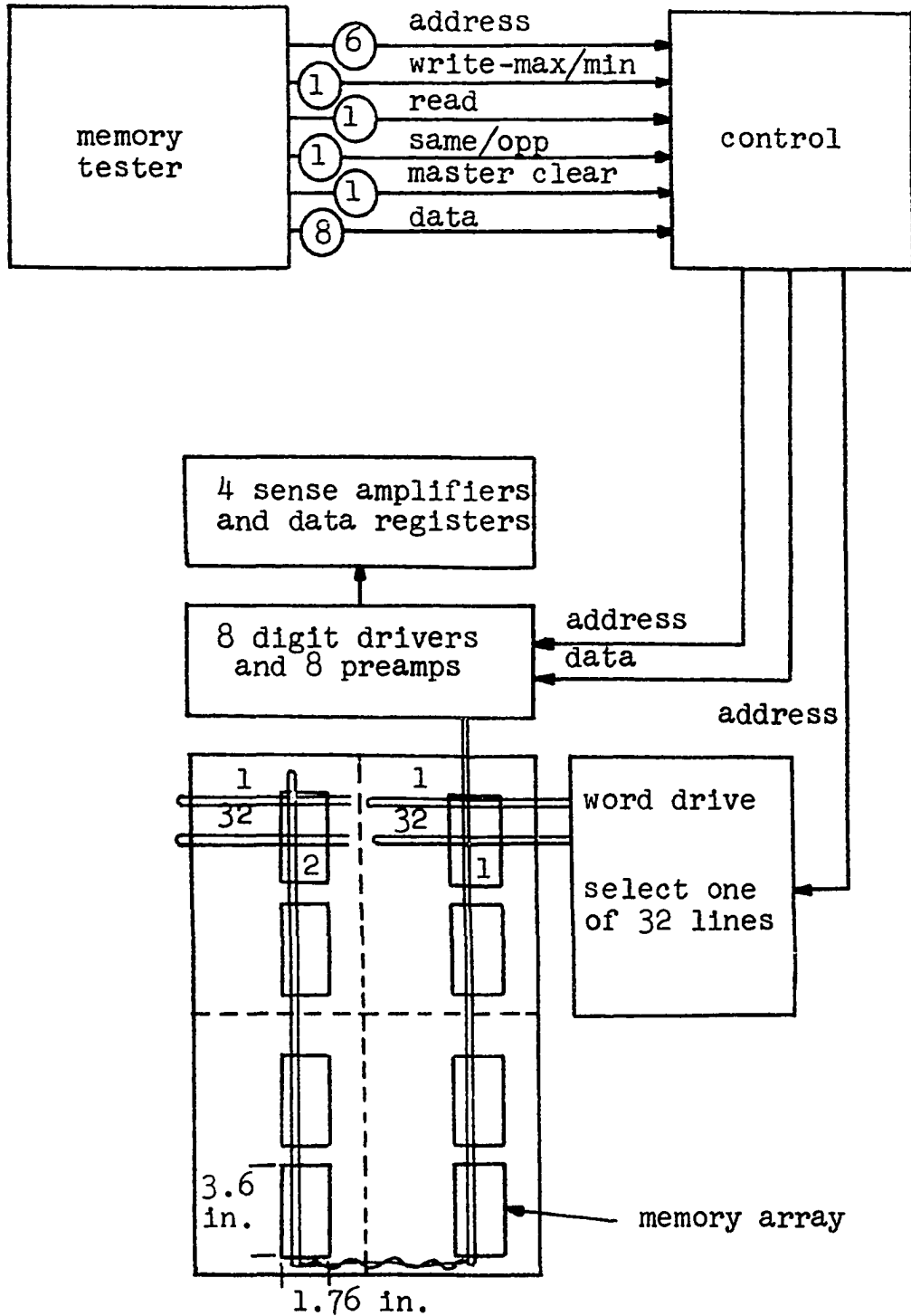


Figure 22. Partially populated memory test system

arrays, as depicted in Figure 22. The entire test plane is capable of holding 32 memory arrays or approximately 10^6 bits.

Word Line Selection

The word access selection scheme, depicted in Figure 23, uses diodes and selection switches to enable one of 32 word lines, organized into a 4 x 8 matrix. An individual word line is enabled by selecting one of four current sources and one of eight current diverters, illustrated in Figure 24. Selection of a word line begins with the enabling of a diverter. A current source is then enabled, once diverter noise has died away. Figure 25 depicts typical read current. Note the 120 nsec delay between diverter selection and the beginning of read current.

Each current source actually consists of two write current sources and a read current source. Write current sources furnish maximum or minimum write current and are enabled by the memory tester. A capacitor, coupling the first and second stages, speeds transistor recovery by removing stored charge. A 300 pf capacitor in read current sources increases read current rise time by overcoming word line inductance. Figure 26 shows ten prehistory current pulses, a single write pulse and ten read pulses, a typical sequence of test pulses in a selected word line.

Word line inductance was 2 uh and resistance 15 Ω .

address and
control

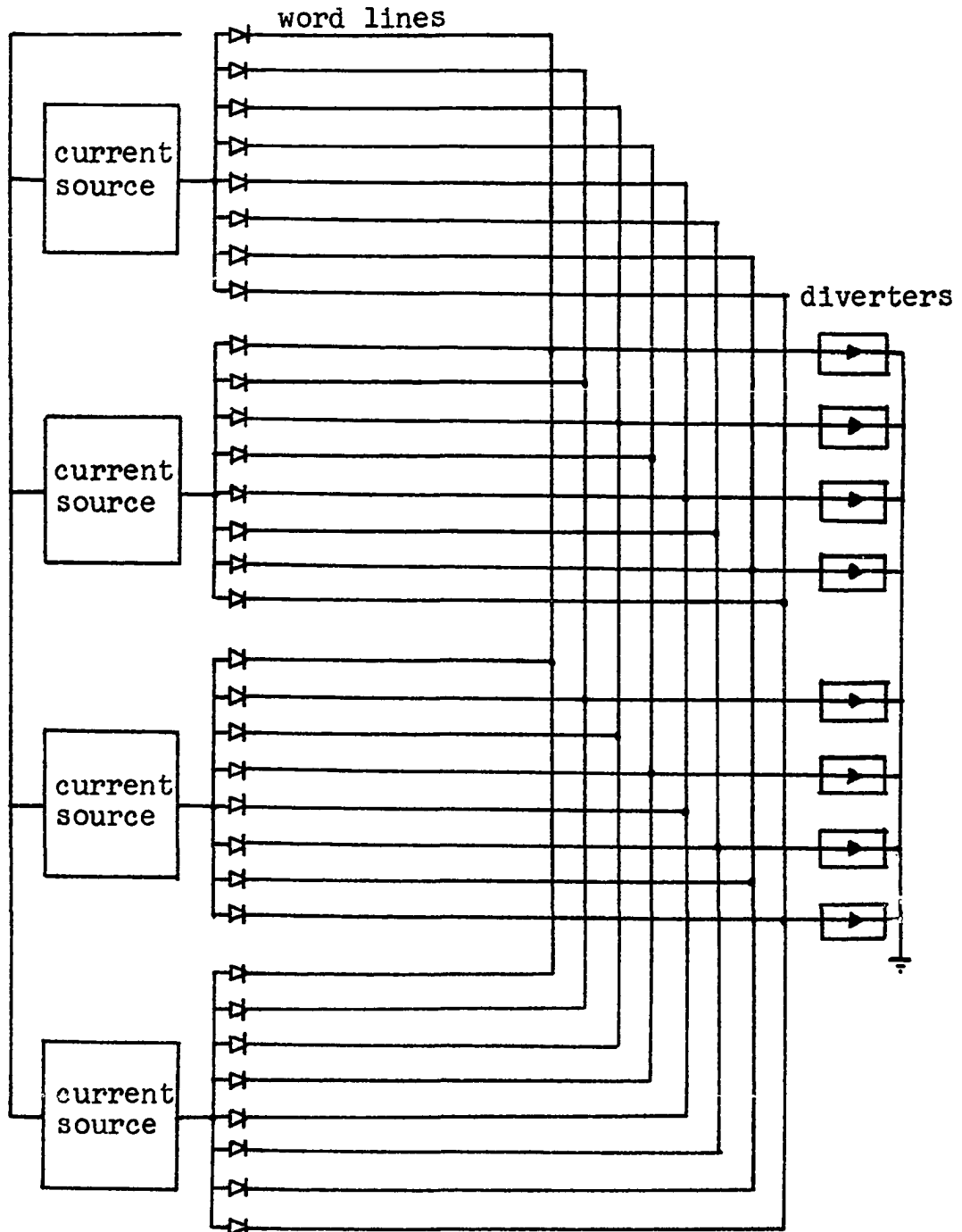


Figure 23. Word access selection scheme

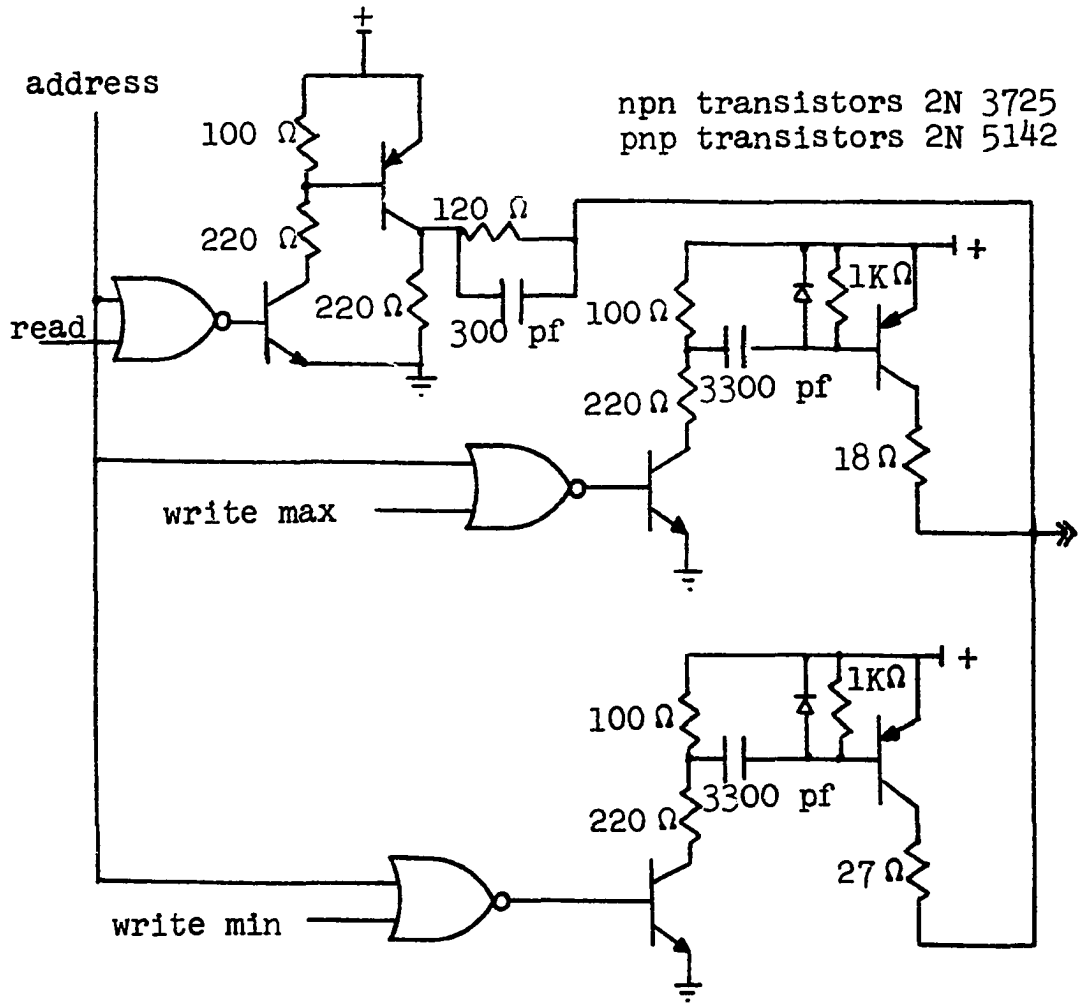


Figure 24A. Read and write current source

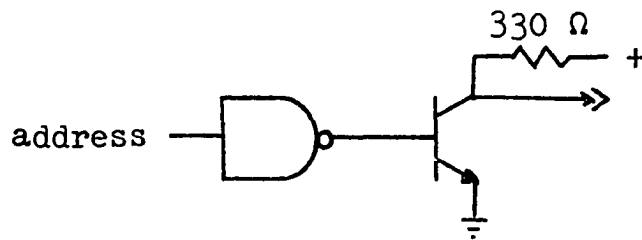


Figure 24B. Diverter switch

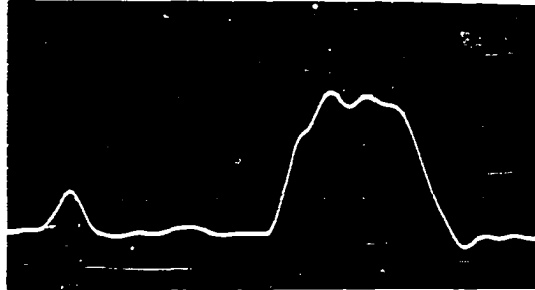


Figure 25. Read current with first pulse indicating current source selection and second pulse diverter selection; vertical scale 40 mA/division; horizontal scale 40 nsec/division

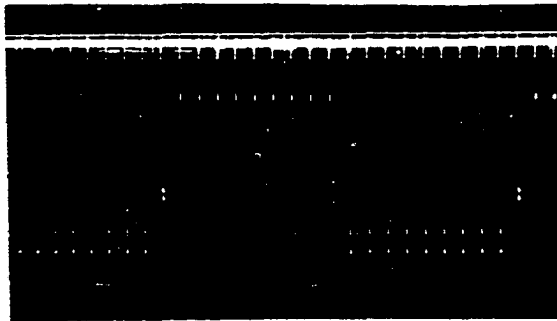


Figure 26. Typical sequence of test current pulses in a selected word line which are prehistory, write, and read; vertical scale 100 mA/division; horizontal scale 20 usec/division

The length of these word lines could be increased to cover more than four film arrays, with a resulting increase in power supply voltage and reduction in sense signal due to a reduction in read current rise time.

The diode selection matrix could be applied to larger selection matrices without much loss of performance. The largest noticeable changes would be a reduction in read current rise time due to increased capacitive loading and greater diverter selection noise, resulting in a longer settling time. Integrated circuits resembling the diverter circuit are available, therefore all circuits with the exception of currents sources, can be contained in standard integrated circuits.

Digit Drivers and Sense Amplifiers

Sense/digit electronics is shown in Figure 27. Four sense amplifiers, eight preamplifiers and eight digit drivers were built to test memory arrays. Two preamplifiers connect to each sense amplifier, however only one preamplifier is activated at any given instant.

Digit electronics is shown transformer coupled to each sense line. Two pairs of TTL open collector IC's, located on either side of the center tapped primary, sink current in one of two directions, establishing bipolar digit current. The primary advantage of transformer coupled digit drive is little sense line loading with the net effect being little

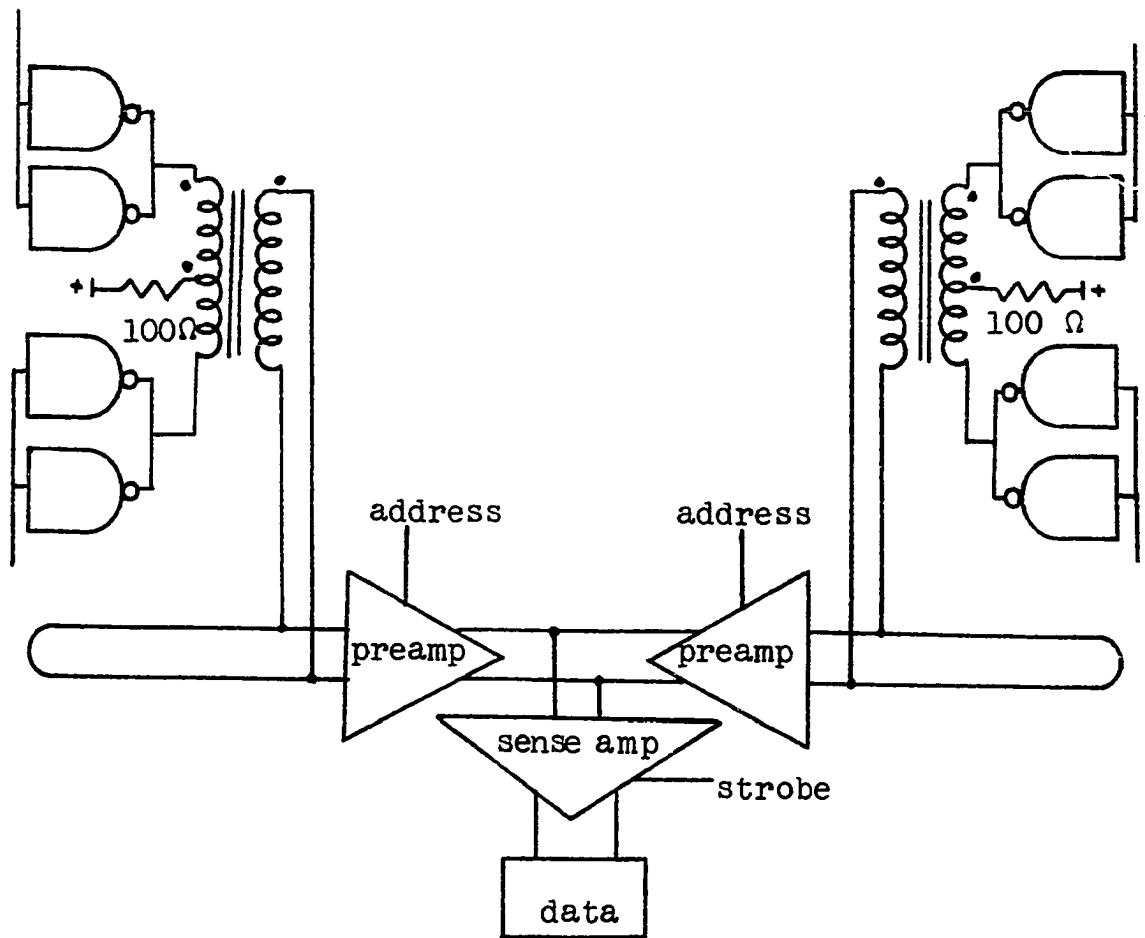


Figure 27. Digit drive and sense circuit

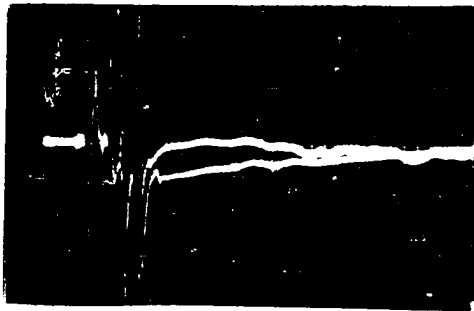


Figure 28. Sense amplifier recovery to unipolar and bipolar digit current; horizontal scale .5 usec/division; vertical scale, 2 V/division

or no reduction in sense signal. Two disadvantages are apparent. First sense/digit cost is increased. Secondly, transformer recovery problems will increase write cycle time. Figure 28 illustrates transformer recovery for unipolar and bipolar digit pulses and Figure 29 shows bipolar digit current and word current. Recovery time is approximately 1.5 usec with unipolar digit current and .4 usec with bipolar current.

An alternate digit circuit is illustrated in Figure 30. Circuit cost and write recovery are improved however sense signal is reduced by approximately one-third. Other disadvantages are a doubling of digit power and the injection of a large common mode voltage on the preamplifier input.

The selection of a digit drive circuit is a difficult problem and is heavily application oriented. Transformer coupled digit drive was chosen for test plane evaluation because it simplified sense amplifier design and did not attenuate sense signal.

Figure 31 illustrates the sense amplifier, data register, strobe circuit. Sense lines are attached to inputs A - A' and B - B'. One of two preamplifiers is selected by enabling a emitter current source. A 11 uh inductor removes any d-c unbalance before it reaches the last stage where strobing occurs. Strobe is applied at the beginning of a read cycle, raising the input of the IC

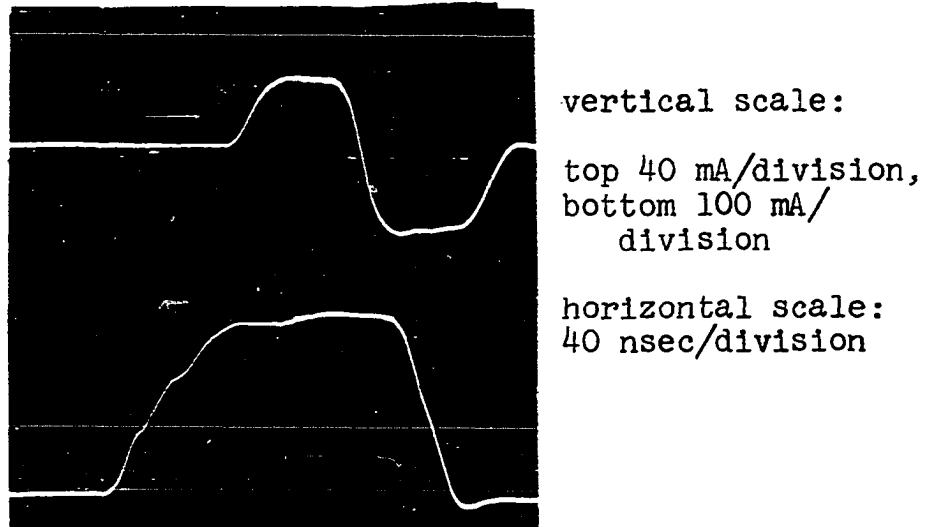


Figure 29. Bipolar digit current and word current

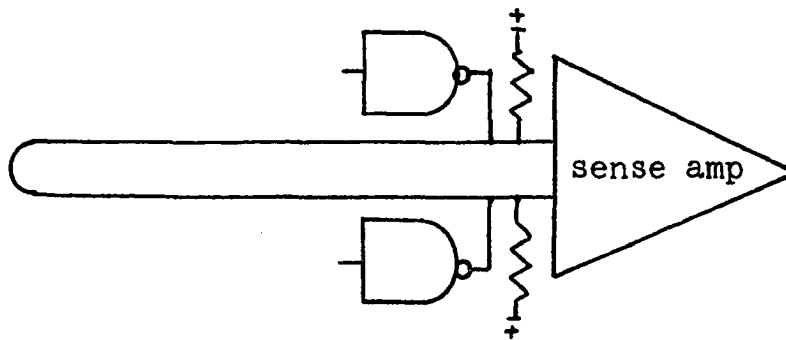


Figure 30. Alternate digit drive circuit

data register to approximately 1.8 V as depicted in Figure 32A. The sense signal, amplified to 900 times its original value, appears at the input of the data register either setting or clearing it, at which time strobe is removed. Figure 32B shows setting of the data register for 1's and 0's.

The transistors used on the input stage were not matched, which proved to be a problem. Fortunately, mismatch could be removed by trimming the $10\ \Omega$ emitter resistors. Mismatch not only lowered gain but also slowed amplifier recovery when preamplifiers were switched. Normal switching time proved to be 150 to 200 ns, which nearly trippled when preamplifiers were mismatched.

Measurements

Figures 33 and 34 show sense amplifier output signals, when strobe is continuously enabled. Note that signals in Figure 33, are approximately 20% lower amplitude than those of Figure 34, because of longer sense lines. Sense lines connecting four film arrays had an average resistance of 45 ohms and a delay of 8 nsec, while the line connecting eight arrays had twice the delay and resistance. Approximately 15% of the signal reduction is attributed to increased sense line delay, the remainder being due to resistance attenuation. Figures 33A, 33B, 34A, and 34B, illustrate signal reduction

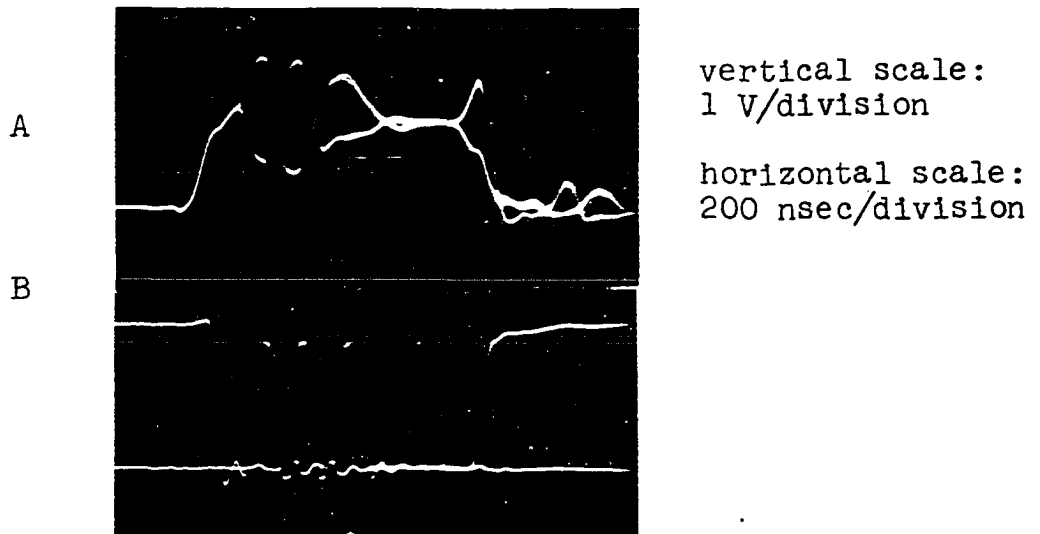


Figure 32. Data register when strobe is enabled

(A) input

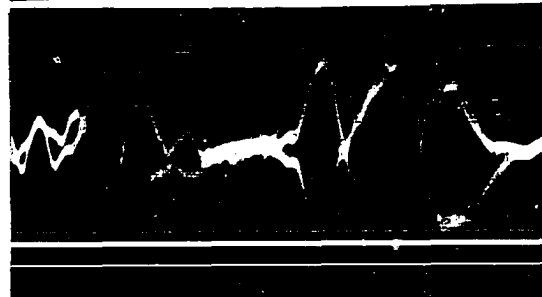
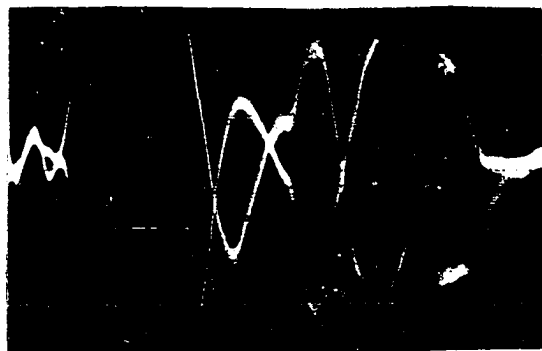
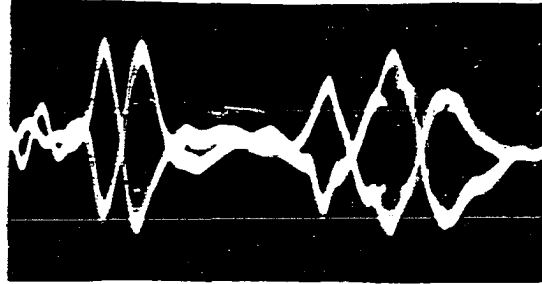
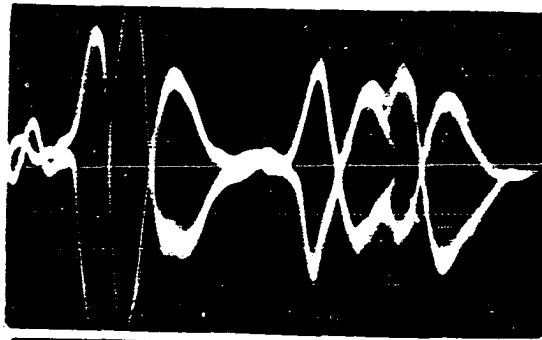
(B) output

Figure 33. Sense amplifier output when sense line connects eight memory arrays; vertical scale, 1 V/division; horizontal scale, 200 nsec/division

- (A) No adjacent disturb test, array number 1 near word drive circuitry is tested
- (B) Adjacent disturb test, array number 1 is tested
- (C) Adjacent disturb test, array number 2 is selected

Figure 34. Sense amplifier output when sense line connects four memory arrays and array number 2 is tested; vertical scale, 1 V/division; horizontal scale, 200 nsec/division

- (A) No adjacent disturb test
- (B) Adjacent disturb test



when the adjacent disturb test is employed with adjacent disturb currents being equal to write currents. The signal reduction suggests an overlapping of adjacent bits which could be eliminated by increasing word line spacing. Note that array number 1 was located approximately 6 in. closer to word drive circuitry than array number 2 and has a shorter preread current settling time because of shorter wire runs.

Figure 35 shows the data register output when the memory was running at 440 nsec in the read-only mode. Read-write cycle time was 1.4 usec which could be reduced if digit circuitry was direct coupled.

Figure 36 illustrates read, write, self disturb and adjacent disturb data. The effect of overlapping adjacent bits is illustrated in the read curve.

An indication of possible operating margins was obtained by setting write and digit current at 250 mA and 45 mA respectively, and then varying read current. The current test pattern contained prehistory, write, adjacent disturb and read currents with write currents set equal. Read current was set at 70 mA and varied by ± 20 mA before loss of information occurred at the data register.

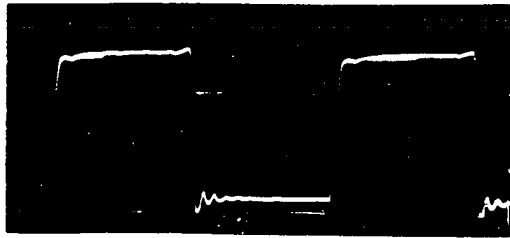


Figure 35. Data register output when memory is cycling in read-only mode at 440 nsec; vertical scale 2 V division; horizontal scale 200 nsec/division

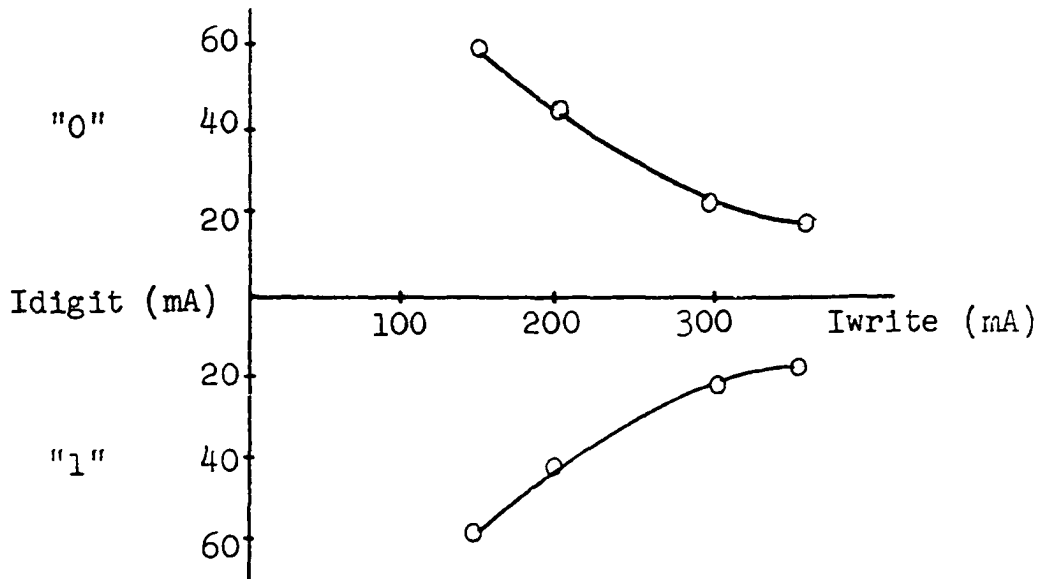


Figure 36A. Write curve for partially populated memory

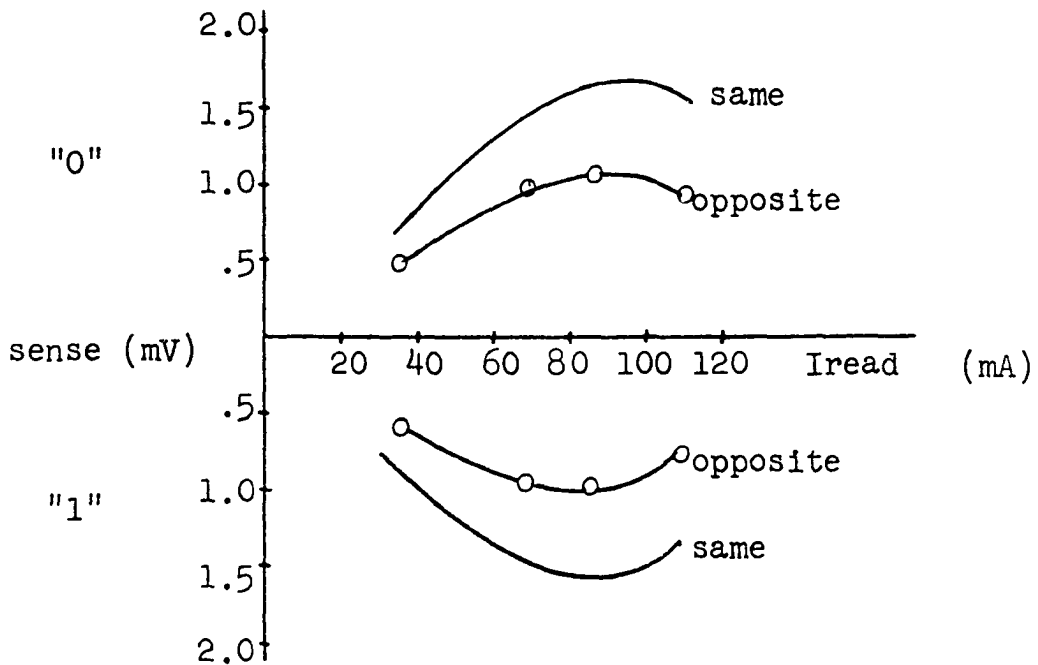


Figure 36B. Read curves for partially populated memory showing output signal when adjacent locations are written in the same and opposite state

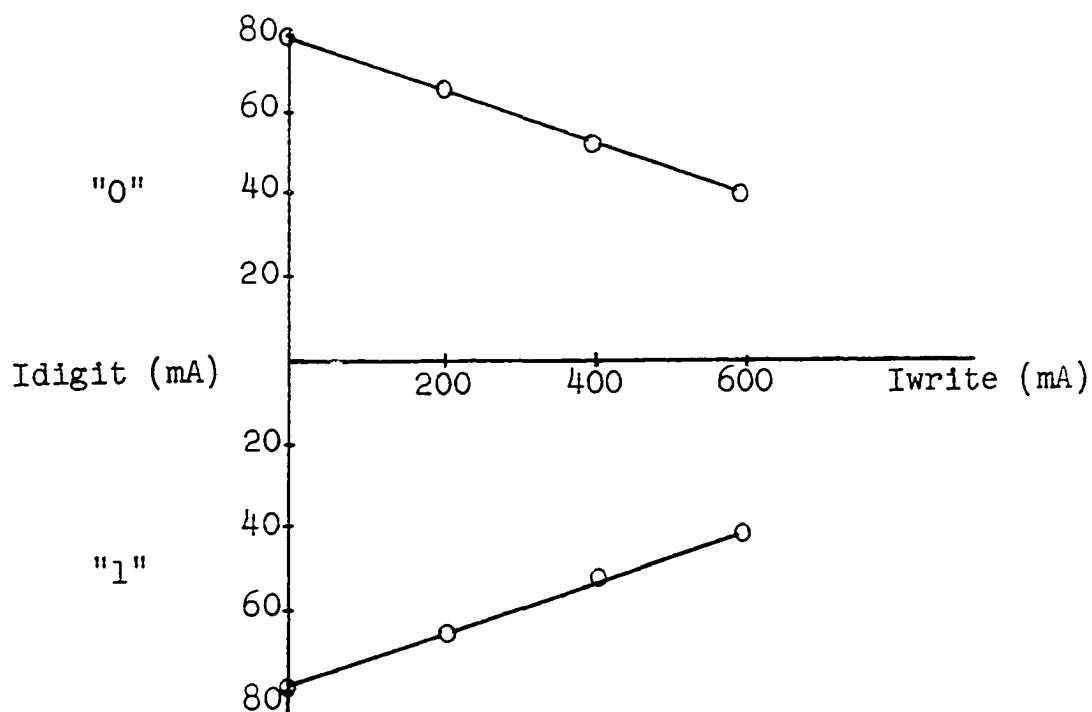


Figure 36C. Adjacent disturb curve for partially populated memory

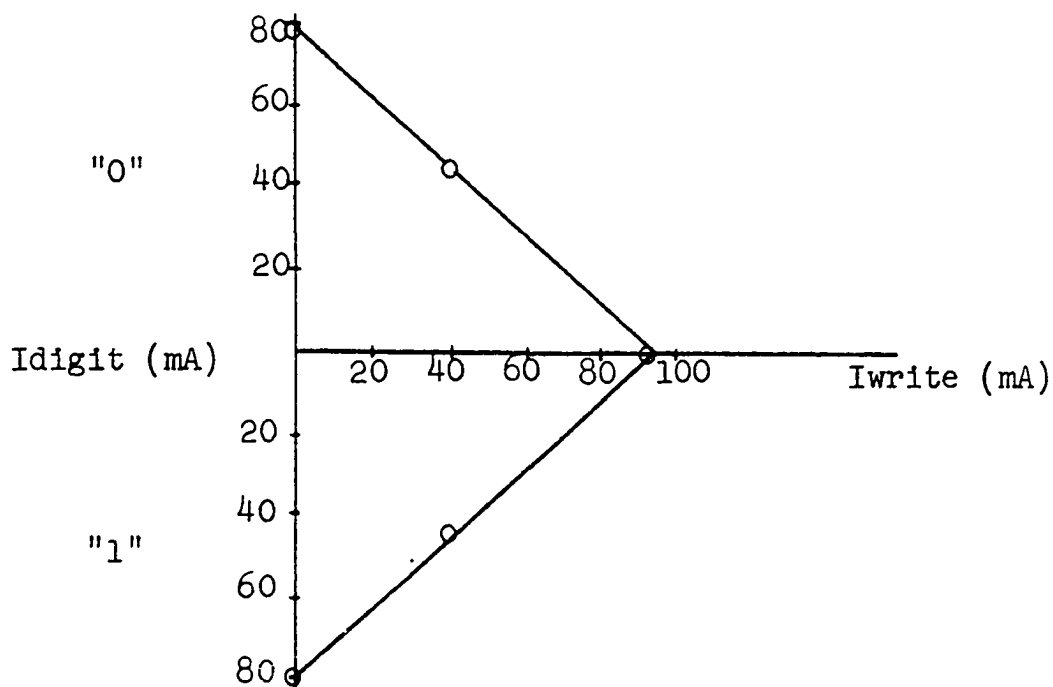


Figure 36D. Self disturb curve for partially populated memory

DISCUSSION AND CONCLUSION

This study has shown that it is possible to construct NDRO film memory arrays having high bit densities, low drive currents that are compatible with integrated circuits and moderate sense signals of 1 mV to 2 mV. A closed flux NDRO element consisting of a magnetically soft Permalloy data film, a magnetically hard NiFe storage film with 20% cobalt doping and an intervening metallic layer was developed for use in a partially populated 10^6 bit memory plane. The memory plane was found to have adequate operating margins while operating with a read only cycle time of 440 nsec.

The fabrication procedure could be improved by using refined techniques however the results obtained indicate that sense signals are large enough to be easily detected using standard techniques. An improved fabrication process could lead to magnetic films having thicknesses of at least $2 \text{ K}\text{\AA}$ with a resulting increase in signal output. Fabrication of thicker sense/digit lines would lower sense/digit line attenuation and could make possible longer sense lines.

It would not be unreasonable to expect a production cost of .4¢/bit to .5¢/bit for a bulk store 10^7 bit NDRO film memory. Of course, a large economic commitment would be required to manufacture arrays in reasonable quantities for such a memory. Electronics cost would be approximately .1¢/bit, assuming the use of low cost epoxy

encased IC's and transistors. Memory arrays should be producible for less than \$40 or .1¢/bit, in production quantities. The greatest portion of memory cost can be attributed to memory stack construction. Winding and termination of multiturn word lines and soldering of sense/digit lines, could cost at least .2¢/bit, assuming the use of mass winding and connection techniques.

ACKNOWLEDGMENTS

The author wishes to thank his major professor, Dr. A. V. Pohm, for suggesting the problem and providing much encouragement and many suggestions. Also, the author wishes to thank members of the staff at Iowa State University who provided many helpful suggestions. Finally, a special word of thanks to his wife for her help in typing the first draft.

REFERENCES

1. Raffel, J. I., "Future Developments in Large Magnetic Film Memories," J. Appl. Phys. 35: 748-753, 1964.
2. Pohm, A. V., J. M. Wang, F. S. Lee, W. Schnasse and T. A. Smay, "High Density Very Efficient Magnetic Film Memory Arrays," IEEE Trans. on Magnetics MAG-5: 408-412, 1969.
3. Pohm, A. V., R. J. Zingg, T. A. Smay, G. A. Watson and R. M. Stewart, Jr., "Size and Speed Capabilities of DRO Film Memories," AIEE Conference Paper, Fall General Meeting, October 1962.
4. Pohm, A. V., "Magnetic Film Scratch Pad Memories," IEEE Trans. on Electronic Computers 15: 542-458, 1966.
5. Janisch, F. R., "Permalloy film NDRO Memory," IEEE Trans. on Magnetic MAG-1: 266-271, 1965.
6. Oakland, L. J. and T. D. Rossing, "Coincident-Current Nondestructive Readout from Thin Magnetic Films," J. Appl. Phys. 30: 543-553, 1959.
7. Olson, C. D., A. L. Scherf, R. W. Heemeyer, et al., "Aerospace Memory Subsystem," Control Data Corp. Government Systems Division Technical Report, November 1967.
8. Petschaver, R. J. and R. O. Tournquist, "A Nondestructive Read Only Memory," WJCC 19: 411-426, 1961.
9. Kohn, G., W. Jutzi, T. Mohr and D. Sertzer, "A Very-High-Speed, Nondestructive-Read Magnetic Film Memory," IBM Journal 1962: 162-167, March 1962.
10. Pohm, A. V., T. A. Smay and W. N. Mayer, "A $.25 \times 10^6$ Bit, High Density, Low Power NDRO Film Memory," IEEE Trans. on Magnetics MAG-3: 481-484, 1967.
11. Raffel, J. E., et al., "A Million Bit Memory Module Using High-Density Batch Fabricated Magnetic Film Arrays," IEEE Trans. on Magnetics MAG-4: 318-319, 1968.
12. Crowther, T. S., "High Density Magnetic Film Memory Techniques," Proc. Inter MAG Conf. 1964: 5.7.1-5.7.6, April 1964.

13. Chang, H., "Coupled Film Memory Elements," J. Appl. Phys. 38: 1203-1204, 1967.
14. Bertelsen, B. I., "Multilayer Processing for Magnetic Film Memory Devices," IEEE Trans. on Magnetics 3: 635-640, 1967.
15. Ahn, K. Y. and J. F. Freedman, "The Effects of Metallic Underlayers on Properties of Permalloy Films," IEEE Trans. on Magnetics 3: 157-162, 1967.
16. Ahn, K. Y. and J. F. Freedman, "Magnetic Properties of Vacuum-Deposited Coupled Films," IBM Journal 1968: 100-109, January 1968.
17. Crowther, T. S., "Specifications and Yields of Composite Magnetic Films for a High Density Memory," IEEE Trans. on Magnetics MAG-4: 529-532, 1968.
18. Chang, H., "Internal Field, Dispersion, Creeping, and Switching Speed of Coupled Films," J. Appl. Phys. 4: 1209-1210, 1963.
19. Crowther, T. S., "The Effect of Cu Diffusion on the Magnetic Properties of NiFe Films," Proc. Intermag Conf., Paper 2.8-1: (1965).
20. Bradley, E. M., "Properties of Magnetic Films for Memory Systems," J. of Appl. Phys. 30: 10513-10573, 1962.
21. Lampert, R. E., J. M. Gorres and M. M. Hanson, "The Magnetic Properties of Co-Ni-Fe-Films," IEEE Trans. on Magnetics MAG-4: 525-528, 1968.
22. Pohm, A. V., L. G. Heller and T. A. Smay, "Adjacent Element Magnetic Coupling on Continuous Film Memories," IEEE Trans. on Magnetics MAG-2: 512-515, 1966.
23. Pohm, A. V. and E. M. Mitchell, "Magnetic Film Memories, A Survey," IRE Trans. on Electronic Computers 1960: 308-314, 1960.